VERTICAL VIBRATION OF A FOUNDATION-SOIL SYSTEM

VERTICAL VIBRATION OF A FOUNDATION-SOIL SYSTEM

BY

WILLIAM JAMES BURWASH, B.ENG.

A Thesis

Submitted to the Faculty of Graduate Studies

in Partial Fulfilment of the Requirements

for the Degree

Master of Engineering

McMaster University

May 1968

MASTER OF ENGINEERING (1968) McMaster University
(Civil Engineering) Hamilton, Ontario

TITLE: Vertical Vibration of a Foundation-Soil System

AUTHOR: William James Burwash, B.Eng. (McMaster Univeristy)

SUPERVISOR: Dr. Michael M.K. Ho

NUMBER OF PAGES: x, 89

SCOPE AND CONTENT: The response of a rigid circular foundation resting on the surface of a cohesionless soil and which is subjected to a constant vertical vibrational force is analyzed experimentally. The response is compared to that predicted analytically. The contact pressure distribution on the foundation-soil interface is used as a means of comparison.

ACKNOWLEDGEMENTS

The author wishes to express his sincere appreciation to Dr. Michael M.K. Ho for his guidance and encouragement throughout the research program. The financial support of the experimental program by the Department of University Affairs, Ontario and by the National Research Council of Canada, Grant Number A-3526 is gratefully acknowledged. The author is grateful for personal financial assistance under a National Research Council postgraduate scholarship.

Technical assistance by Messrs. John Myers, Jim Meyer, Jim Bryson and Rui Lopes is gratefully acknowledged. Gratitude is extended to Miss Suzanne Chatland who typed the manuscript and assisted in its preparation. The interest and suggestions of Mr. C. T. Hwang are appreciated.

TABLE OF CONTENTS

LIST OF FIGURES

LIST OF TABLES

LIST OF PHOTOGRAPHS

NOMENCLATURE

A	amplitude factor
A_{max}	maximum amplitude factor
A_c	contact area of foundation
a_o	frequency factor
b	mass ratio
C_c	compressive wave velocity
C_s	shear wave velocity
e	base of natural logarithms, 2.7182....
e	void ratio
f_o	resonant frequency
f	frequency
f_1, f_2	displacement function
G	shear modulus
i	$\sqrt{-1}$
m_o	mass of foundation
p	pressure
Q	input force
Q_1	amplitude of input force
R	soil reaction force
R_1	amplitude of soil reaction force
r	radius
r_o	radius of foundation
t	time
W	weight of foundation
X	amplitude of vibration
X_{max}	maximum amplitude of vibration

x	displacement of foundation
κ	confining pressure factor
ν	Poisson's ratio
ρ	mass density of soil
ϕ_{Q-R}	phase shift between input force and soil reaction
ϕ_{Q-x}	phase shift between input force and displacement
ϕ_{x-R}	phase shift between displacement and soil reaction
σ_c	confining pressure
ω	angular frequency

CHAPTER 1

INTRODUCTION

Vibration effects on foundations have become of increasing importance in recent years in both research and engineering practice. Among the many proposed theories for the analysis of foundation vibrations, the Reissner-Sung elastic half-space theory has often been considered and utilized. There is, however, a deficiency of test results obtained from either the field or laboratory to verify the validity and applicability of the Reissner-Sung theory. This thesis presents the results of laboratory tests in an attempt to clarify this problem.

The use of the Reissner-Sung theory to predict the amplitude of vibration and resonant frequency requires, among other factors, a knowledge of the dynamic contact pressure distribution at the foundation-soil interface. For this reason, the investigation reported herein includes the determination of the magnitude and phase relations of the dynamic contact pressure as well as the force-displacement characteristics.

A rigid circular foundation, six inches in diameter, was constructed of steel. Pressure transducers were mounted flush with the base of the footing at varying radii. The footing rests on the surface of dense Ottawa sand contained in a bin four and one-half feet square and thirty inches deep. The bin was lined with styrofoam to avoid reflection of energy waves. The footing is subject to a steady-state vertical vibration of constant force amplitude. A force

link was used to ensure a constant input force and a displacement transducer was used to measure the amplitude of vibration as a function of frequency. Signals from the six pressure transducers, the input force and the displacement transducers were recorded simultaneously while their phase relations were measured by means of a phase meter.

Results are presented for foundations of five different mass ratios. By use of the displacement functions the compatibility of the results is checked. The results are compared with those predicted by the Reissner-Sung theory. The dynamic pressure distribution is used as a means of comparison.

CHAPTER 2

LITERATURE REVIEW

There are in general two methods of analyzing vibratory foundation-soil systems. The first method assumes that the system can be represented by a mass-spring-dashpot system. This method was investigated notably by Hertwig, Früh, and Lorenz (1933), Crockett and Hammond (1948), and Pauw (1953). The difficulty with this method is the determination of the mass of soil vibrating in phase with the foundation and the determination of the appropriate damping factor. It was found that the in-phase mass and damping factor were functions of frequency, magnitude of force, and size and weight of the foundation.

A second approach is the elastic half-space method. This method is adopted throughout this thesis. It is assumed that the soil can be represented as a homogeneous, isotropic, semi-infinite elastic medium. Reissner (1936) investigated the problem of a rigid circular mass subjected to a constant vertical harmonic force. The solution assumed a uniform pressure distribution on the interface of the foundation-soil system. Sung (1953) extended the work of Reissner by assuming parabolic and rigid base as well as uniform pressure distributions. Sung included both a constant force and a frequency dependent force in his analysis. Richart (1961) presented the results of Sung in a form more suitable to practicing engineers and this form has become of increasing popularity.

Different modes of vibration have also been analyzed using the elastic half-space method. Arnold, Bycroft, and Warburton (1955) investigated vertical and horizontal translation as well as torsion and rocking. Their analysis included a finite depth as well as an infinite depth of elastic body. The solution concerning the finite depth of stratum was left in integral form. The authors supported their analysis with laboratory experiments performed on foam rubber.

Warburton (1957) evaluated the integral given by Arnold, Bycroft and Warburton for the case of a vertical force acting upon an elastic body of infinite surface area and finite depth. His solution showed that for shallow stratums higher values of resonant frequency and amplitude of vibration occurred than that for a semi-infinite body. He also stated that for a depth of stratum greater than six times the diameter of the footing the resonant frequency was independent of the depth of stratum.

Hardin and Richart (1963) performed laboratory tests to determine the compressive and shear wave velocities of Ottawa sand, crushed quartz sand, and crushed quartz silt. The tests were performed to determine the effects of confining pressure, water content, void ratio, and grain size distribution. The effects of grain size distribution and water content for sands was found to be negligible. The effect of time and consolidation was significant for the silt. Empirical

equations dependent upon the void ratio and confining pressure were developed for the shear wave velocity in the sands.

Hall and Richart (1963) investigated the effect of amplitude of vibration on the shear and compressive wave velocities of Ottawa sand, glass beads, and crushed quartz silt. The tests showed that the shear and compressive wave velocities decreased as the amplitude of vibration increased.

A comprehensive field investigation of foundation vibrations has been conducted by the U.S. Army Engineer Waterways Experiment Station and the results have been reported by Fry (1963). The foundations were circular reinforced concrete pads of varying weight and radius and rested upon the surface of the soil. The effect of the type of soil was studied by conducting tests on a cohesive and on a cohesionless soil. Steady-state vibrations were applied in the vertical, torsional and rocking modes. The elastic properties of the soils were determined by seismic methods.

Whitman (1966) and Richart and Whitman (1967) have reported analyses of these tests. The results were compared with the predictions of the elastic half-space method. The results compared favourably qualitatively and quantitatively. A greater scatter of results occurred for the cohesionless than for the cohesive soil. The results of the tests performed on the cohesive soil corresponded with the predictions for a rigid base pressure distribution while the tests on the cohesionless soil corresponded to the parabolic pressure distribution.

Chae (1964) investigated experimentally the pressure distribution beneath a circular footing subjected to a constant vertical vibratory force. The footing rested on the surface of densely compacted Ottawa sand. The footing consisted of concentric rings connected to a rigid upper plate by means of load cells which allowed measurements of pressure. It was found that the pressure varied in phase and magnitude across the radius of the footing and that it was frequency dependent. Chae also measured the amplitude of vibration as a function of frequency for footings of different weight and presented his results in the same form as that of Sung. The results compared favourably within the range of the resonant frequencies encountered.

Lysmer and Richart (1966) extended the work of Sung and Reissner to include the high frequency range for vertical vibration. The analysis includes steady-state vibrations and arbitrary pulse loading. Good agreement was obtained between their analysis and experimental results published by Fry (1963) and Drnevich, Hall and Richart (1966).

The dynamic pressure distribution on the contact surface of a foundation-soil system is relatively unknown. This point has been emphasized recently by Richart and Whitman (1967). If the dynamic pressure distribution is known, then it can be compared with the three assumed pressure distributions of the Reissner-Sung theory. A comparison can then be made to determine the reliability of the analytical method. This comparison is presented in this thesis.

CHAPTER 3

THE REISSNER-SUNG THEORY

An analytical solution for the steady-state vibration of a foundation resting upon the surface of a semi-infinite, isotropic, homogeneous, elastic body has been investigated by Reissner (1936). His solution is limited to a rigid circular mass subjected to a vertical harmonic force. Reissner's solution assumes a uniform contact pressure distribution. Sung (1953) extended Reissner's work to include parabolic and rigid base pressure distribution.

A mathematical model of the foundation-soil system is represented in Figure 1. It is assumed that the soil can be represented as a semi-infinite, isotropic,homogeneous, elastic body. The footing is axially symmetric and absolutely rigid thus producing uniform displacement beneath the footing. It is assumed that there are no shear stresses acting on the foundation soil interface. The periodic force acts through the centre of gravity of the footing.

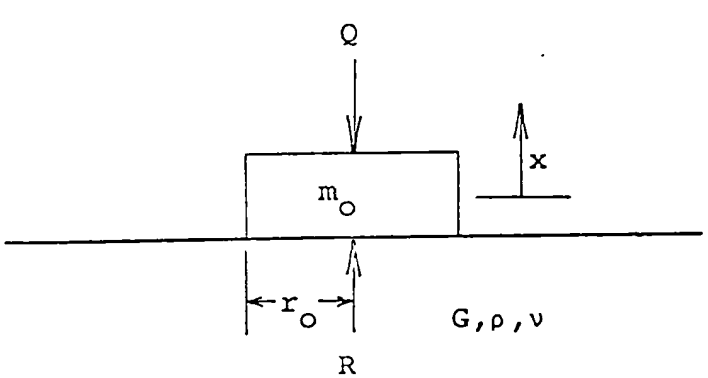

Figure 1. MATHEMATICAL MODEL OF FOUNDATION-SOIL SYSTEM

The equation of motion of the system can be expressed by the following:

$$m_o\ddot{x} = R - Q \tag{1}$$

$$= R_1 e^{i\omega t} - Q_1 e^{i(\omega t + \phi_{Q-R})} \tag{2}$$

where

m_o = mass of foundation

x = displacement of footing

Q = input force having amplitude Q_1

R = soil reaction force having amplitude R_1

ω = angular frequency

ϕ_{Q-R} = phase difference between input force and soil reaction

$i = \sqrt{-1}$

$e = 2.71828.....$

The solution to this problem as developed by Reissner and Sung is

$$x = \frac{R_1}{r_o G} (f_1 + if_2)\, e^{i\omega t} \tag{3}$$

where

f_1, f_2 = displacement functions

G = shear modulus of soil

The acceleration can be determined from equation (3) by differentiation

$$\ddot{x} = \frac{-R_1\omega^2}{r_o G} (f_1 + if_2)\, e^{i\omega t} \tag{4}$$

Substitution of equation (4) in equation (2) yields

$$\frac{-R_1\omega^2 m_o}{r_o G}(f_1 + if_2)\, e^{i\omega t} = R_1 e^{i\omega t} - Q_1 e^{i(\omega t + \phi_{Q-R})} \quad (5)$$

Simplification of the above expression is achieved by the introduction of two dimensionless parameters. One parameter is the frequency factor, a_o, defined as

$$a_o = \omega r_o \sqrt{\frac{\rho}{G}} \quad (6)$$

where

ρ = density of soil

The other parameter is the mass ratio, b, defined as

$$b = \frac{m_o}{\rho r_o^3} \quad (7)$$

By substitution of equations (6) and (7) in equation (5) the result is

$$-R_1 a_o^2\, b(f_1 + if_2)\, e^{i\omega t} = R_1 e^{i\omega t} - Q_1 e^{i(\omega t + \phi_{Q-R})}$$

or

$$-R_1 a_o^2\, b(f_1 + if_2) = R_1 - Q_1 e^{i\phi_{Q-R}} \quad (8)$$

Two equations are formed by taking the real and imaginary parts respectively.

$$-R_1 a_o^2 b f_1 = R_1 - Q_1 \cos \phi_{Q-R} \quad (9)$$

$$R_1 a_o^2 b f_2 = Q_1 \sin \phi_{Q-R} \quad (10)$$

From equations (9) and (10) the following relationship is derived

$$\tan \phi_{Q-R} = \frac{b\, a_o^2 f_2}{1 + b\, a_o^2 f_1} \quad (11)$$

By applying equation (11) in equation (10) the following relationship can be derived

$$R_1 = \frac{Q_1}{\sqrt{(1 + ba_o^2 f_1)^2 + (ba_o^2 f_2)^2}} \tag{12}$$

From equation (3) it follows that

$$\phi_{R-x} = \tan^{-1} - \frac{f_2}{f_1} \tag{13}$$

By substitution of equations (12) and (13) in (3) and the results arranged such that

$$x = X\, e^{i(\omega t + \phi_{x-R})} \tag{14}$$

it is found that

$$X = \frac{Q_1}{r_o G} \sqrt{\frac{f_1^2 + f_2^2}{(1 + ba_o^2 f_1)^2 + (ba_o^2 f_2)^2}} \tag{15}$$

From the phase angle relations it is known that

$$\phi_{Q-x} = \phi_{Q-R} + \phi_{R-x} \tag{16}$$

Thus

$$\tan \phi_{Q-x} = \tan (\phi_{Q-R} + \phi_{R-x})$$

$$= \frac{-f_2}{f_1 + ba_o^2 (f_1^2 + f_2^2)} \tag{17}$$

The Displacement Functions

The displacement functions are dependent upon the frequency factor, Poisson's ratio of the soil, and the type of pressure distribution. Reissner (1936) determined the displacement functions assuming uniform pressure distribution. Sung (1953) extended his solution for parabolic and rigid base pressure distribution. The stress distributions assumed

by Sung are given as follows:

(i) Rigid Base Pressure Distribution

$$p(r,t) = \frac{Q_1 e^{i\omega t}}{2\pi r_o \sqrt{r_o^2 - r^2}} \quad \text{for } r < r_o$$
$$= 0 \quad \text{for } r > r_o \tag{18}$$

(ii) Uniform Pressure Distribution

$$p(r,t) = \frac{Q_1 e^{i\omega t}}{\pi r_o^2} \quad \text{for } r < r_o$$
$$= 0 \quad \text{for } r > r_o \tag{19}$$

(iii) Parabolic Pressure Distribution

$$p(r,t) = \frac{2\, Q_1 e^{i\omega t}}{\pi r_o^4} \quad \text{for } r < r_o$$
$$= 0 \quad \text{for } r > r_o \tag{20}$$

where

p = pressure

r_o = radius of foundation

r = radius of any point on foundation

The displacement functions determined by Sung are shown as a power series representation in Tables I and II and in graphical form in Figure 2. Sung limited his analysis for $0<a_o<1.5$ for which he assumed the pressure distribution to be independent of frequency.

Resonant Frequency and Maximum Amplitude of Vibration

The amplitude of vibration can now be determined as a function of frequency. Equation (15) can be expressed

POWER SERIES REPRESENTATION OF THE FUNCTION $-f_1$ (After Sung)

Rigid Base	$\nu = 0$	$-f_1 = 0.250000 - 0.109375\, a_o^2 + 0.010905\, a_o^4 - \ldots + \ldots$
	$\nu = 1/4$	$-f_1 = 0.187500 - 0.070313\, a_o^2 + 0.006131\, a_o^4 - \ldots + \ldots$
	$\nu = 1/3$	$-f_1 = 0.166667 - 0.060764\, a_o^2 + 0.005085\, a_o^4 - \ldots + \ldots$
	$\nu = 1/2$	$-f_1 = 0.125000 - 0.046875\, a_o^2 + 0.003581\, a_o^4 - \ldots + \ldots$
Uniform	$\nu = 0$	$-f_1 = 0.318310 - 0.092841\, a_o^2 + 0.007405\, a_o^4 - \ldots + \ldots$
	$\nu = 1/4$	$-f_1 = 0.238733 - 0.059683\, a_o^2 + 0.004163\, a_o^4 - \ldots + \ldots$
	$\nu = 1/3$	$-f_1 = 0.212207 - 0.051578\, a_o^2 + 0.003453\, a_o^4 - \ldots + \ldots$
	$\nu = 1/2$	$-f_1 = 0.159155 - 0.039789\, a_o^2 + 0.002432\, a_o^4 - \ldots + \ldots$
Parabolic	$\nu = 0$	$-f_1 = 0.424414 - 0.074272\, a_o^2 + 0.004232\, a_o^4 - \ldots + \ldots$
	$\nu = 1/4$	$-f_1 = 0.318310 - 0.047747\, a_o^2 + 0.002379\, a_o^4 - \ldots + \ldots$
	$\nu = 1/3$	$-f_1 = 0.282942 - 0.041262\, a_o^2 + 0.001973\, a_o^4 - \ldots + \ldots$
	$\nu = 1/2$	$-f_1 = 0.212207 - 0.031831\, a_o^2 + 0.001389\, a_o^4 - \ldots + \ldots$

TABLE II

POWER SERIES REPRESENTATION OF THE FUNCTION f_2 (After Sung)

Rigid Base	$\nu = 0$	$f_2 = 0.214474\ a_o - 0.039416\ a_o^3 + 0.002444\ a_o^5 - \ldots + \ldots$
	$\nu = 1/4$	$f_2 = 0.148594\ a_o - 0.023677\ a_o^3 + 0.001294\ a_o^5 - \ldots + \ldots$
	$\nu = 1/3$	$f_2 = 0.130630\ a_o - 0.020048\ a_o^3 + 0.001052\ a_o^5 - \ldots + \ldots$
	$\nu = 1/2$	$f_2 = 0.104547\ a_o - 0.014717\ a_o^3 + 0.000717\ a_o^5 - \ldots + \ldots$
Uniform	$\nu = 0$	$f_2 = 0.214474\ a_o - 0.029561\ a_o^3 + 0.001528\ a_o^5 - \ldots + \ldots$
	$\nu = 1/4$	$f_2 = 0.148594\ a_o - 0.017757\ a_o^3 + 0.000808\ a_o^5 - \ldots + \ldots$
	$\nu = 1/3$	$f_2 = 0.130630\ a_o - 0.015037\ a_o^3 + 0.000658\ a_o^5 - \ldots + \ldots$
	$\nu = 1/2$	$f_2 = 0.104547\ a_o - 0.011038\ a_o^3 + 0.000444\ a_o^5 - \ldots + \ldots$
Parabolic	$\nu = 0$	$f_2 = 0.214474\ a_o - 0.019708\ a_o^3 + 0.000764\ a_o^5 - \ldots + \ldots$
	$\nu = 1/4$	$f_2 = 0.148594\ a_o - 0.011837\ a_o^3 + 0.000405\ a_o^5 - \ldots + \ldots$
	$\nu = 1/3$	$f_2 = 0.130630\ a_o - 0.010024\ a_o^3 + 0.000328\ a_o^5 - \ldots + \ldots$
	$\nu = 1/2$	$f_2 = 0.104547\ a_o - 0.007358\ a_o^3 + 0.000222\ a_o^5 - \ldots + \ldots$

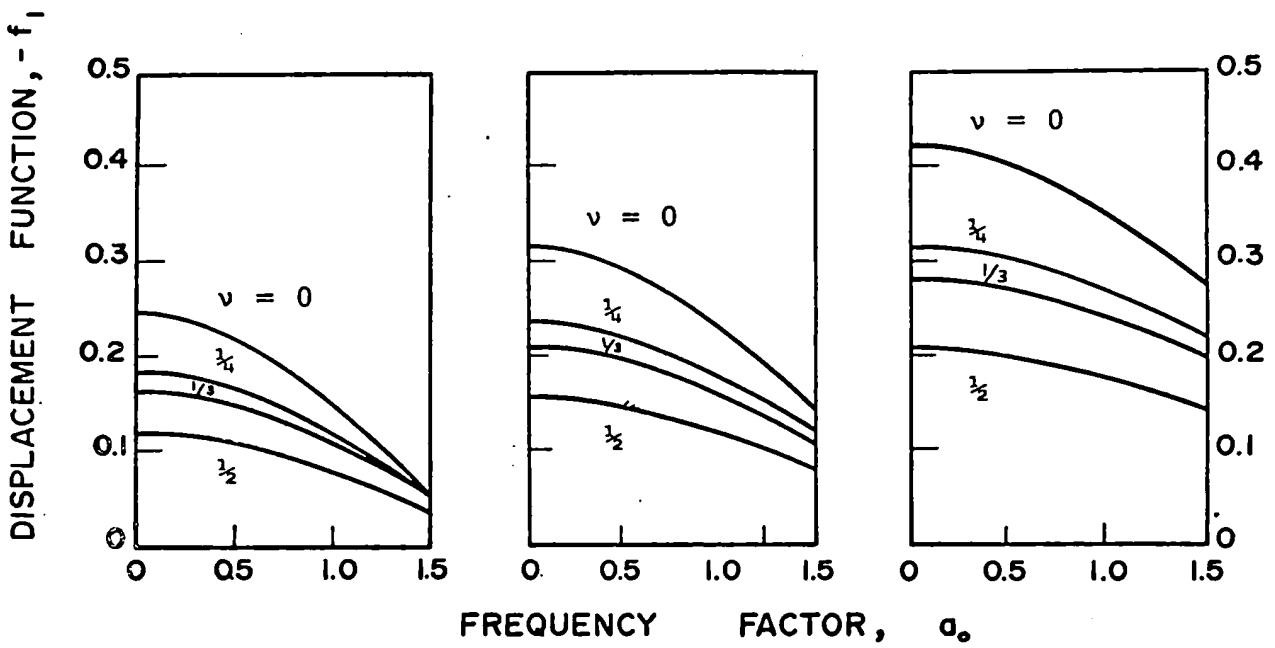

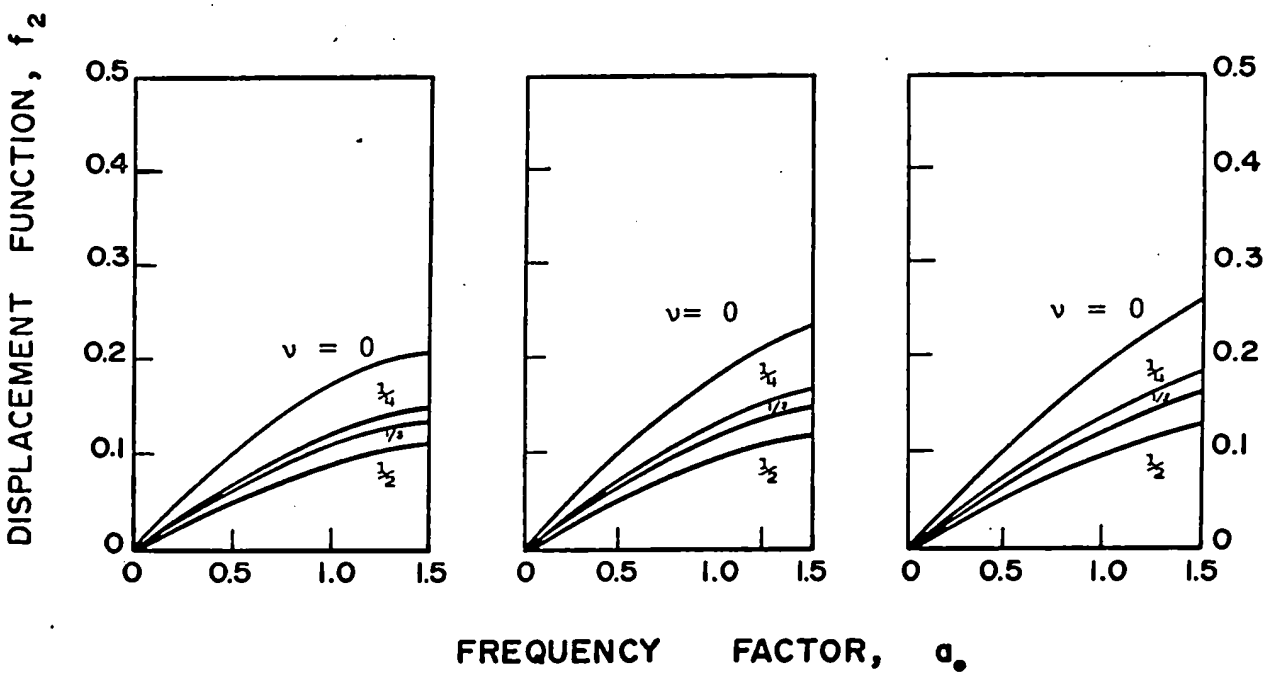

FIG. 2 DISPLACEMENT FUNCTIONS, f_1 & f_2 (AFTER SUNG)

in dimensionless form

$$\frac{XGr_o}{Q_1} = \sqrt{\frac{f_1^2 + f_2^2}{(1 + ba_o^2 f_1)^2 + (ba_o^2 f_2)^2}} \tag{21}$$

The right hand portion of equation (21) is defined as

$$A = \sqrt{\frac{f_1^2 + f_2^2}{(1 + ba_o^2 f_1)^2 + (ba_o^2 f_2)^2}} \tag{22}$$

where A is termed the amplitude factor. The maximum value of A is termed A_{max} and occurs at the resonant frequency of the foundation.

For a given foundation, the mass ratio is defined and is a constant. Amplitude-frequency relations can then be determined by varying the frequency factor and knowing the relation between the displacement functions and the frequency factor. Figure 3 shows the amplitude-frequency relations for different mass ratios assuming a parabolic pressure distribution and Poisson's ratio of 1/3.

The resonant frequency and maximum amplitude of vibration can be determined from Figure 3 by the following equation if the soil properties are known.

$$X_{max} = \frac{Q_1}{r_o G} A_{max} \tag{23}$$

The value of the frequency factor for which the maximum amplitude occurs defines the resonant frequency, f_o.

$$f_o = \frac{a_o}{2\pi r_o} \sqrt{\frac{G}{\rho}} \tag{24}$$

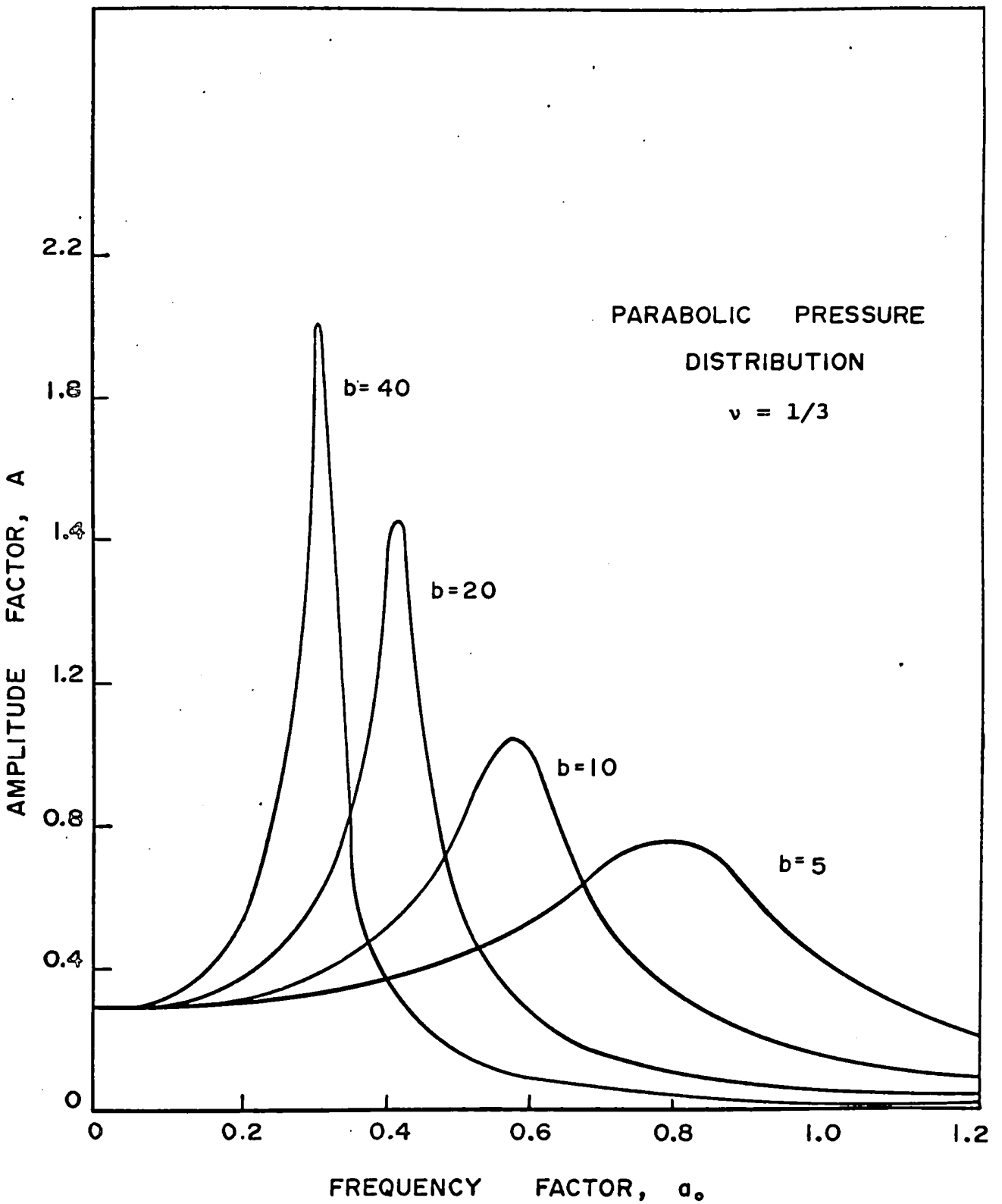

FIG. 3 AMPLITUDE FACTOR VS. FREQUENCY FACTOR

Determination of the resonant frequency and maximum amplitude of vibration for mass ratios not shown in Figure 3 require interpolation. Richart (1960) presented Sung's results in a form more useful to practising engineers. Richart limited his analysis to the rigid base pressure distribution.

Figures 4 and 5 are in similar form to that used by Richart but are presented for parabolic pressure distribution. Figure 4 may be used to determine the resonant frequency. For a given value of b, a_o is determined for a given value of Poisson's ratio. The resonant frequency can then be determined using equation (24). Figure 5 may be used to determine the maximum amplitude of vibration. For a given value of b, A_{max} is determined for a given value of Poisson's ratio. The maximum amplitude of vibration can then be determined using equation (23). The results shown in Figures 3, 4, and 5 were calculated with an IBM 7040 computer using Sung's displacement functions.

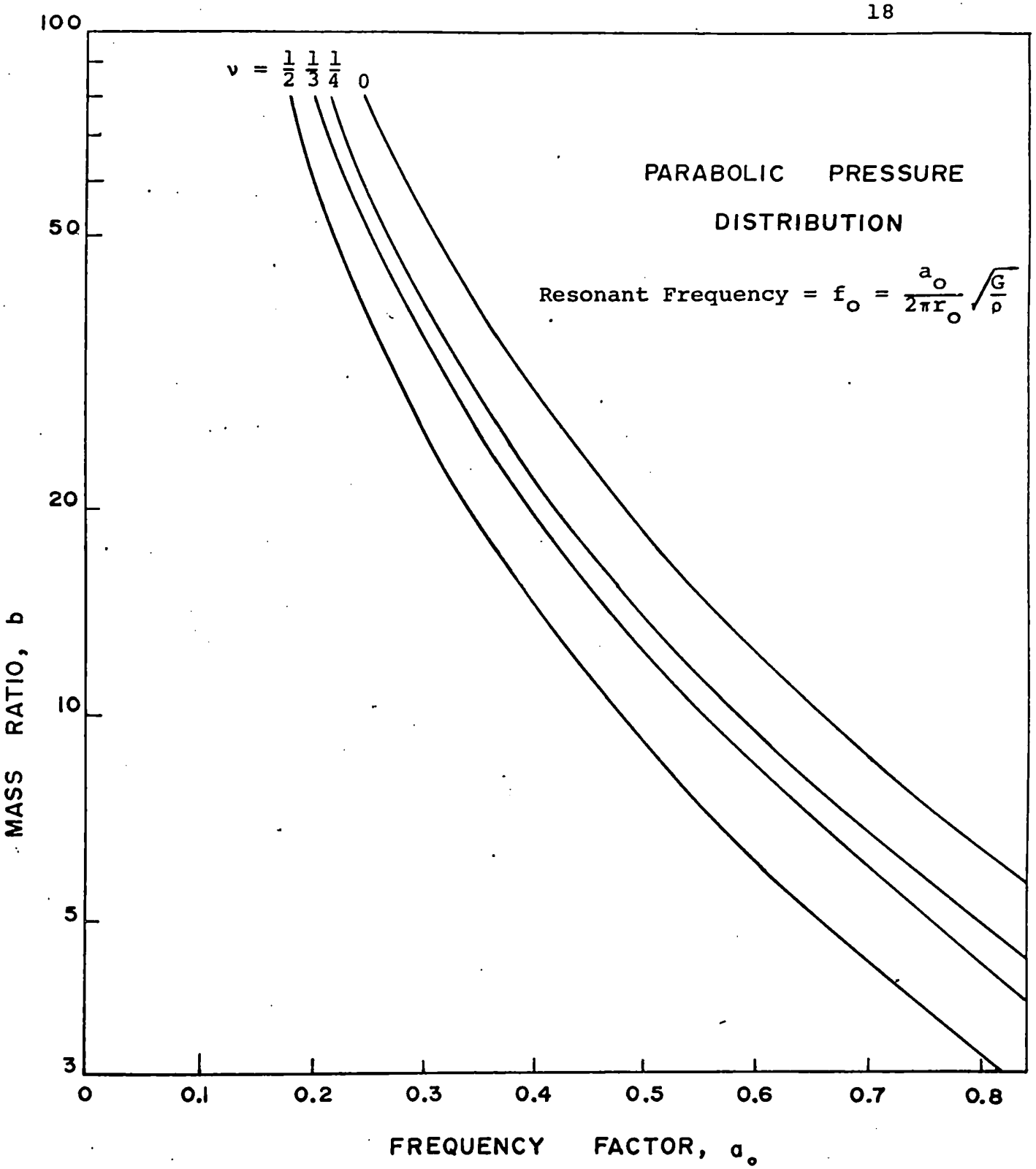

FIG. 4 MASS RATIO VS. FREQUENCY FACTOR

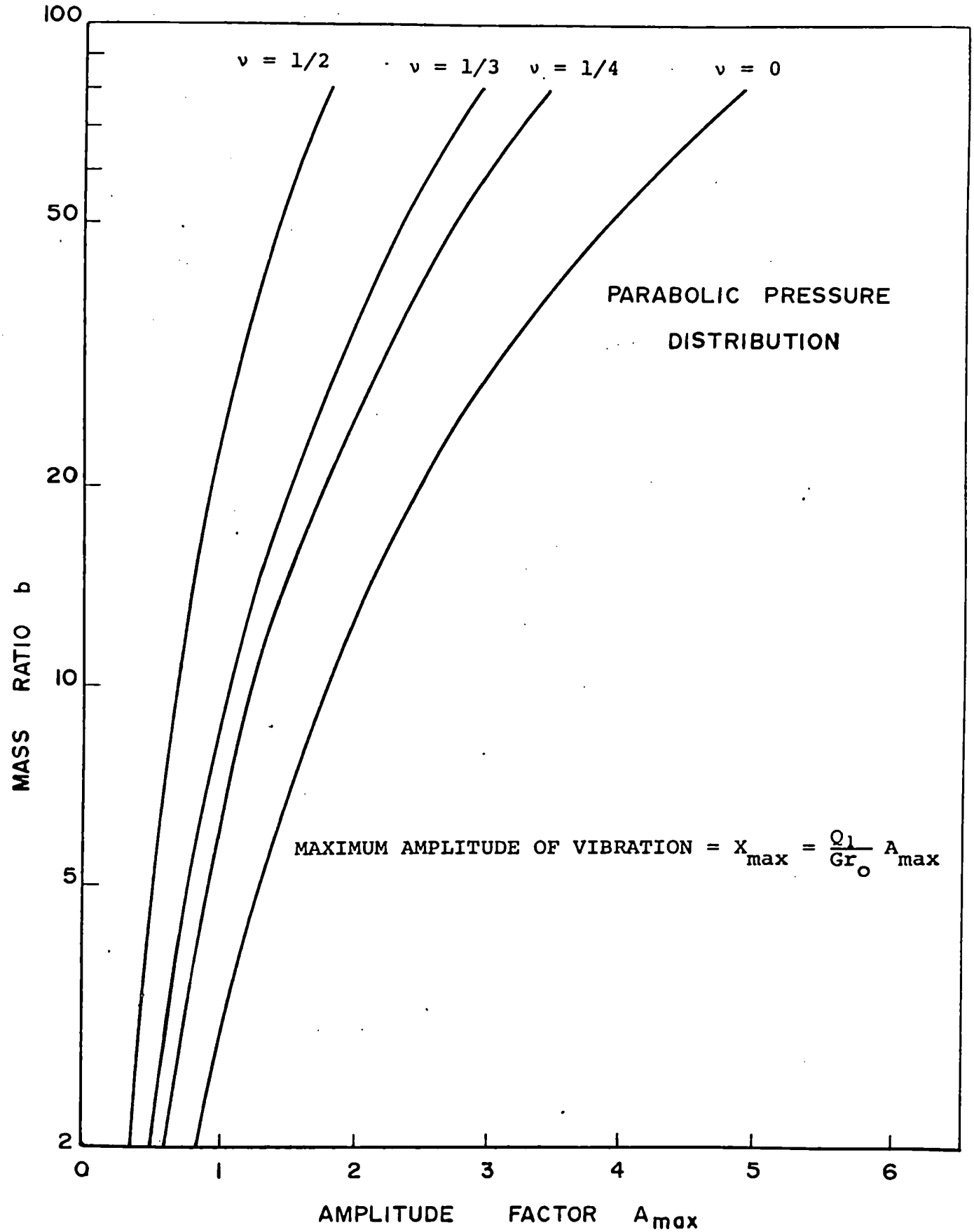

FIG. 5 MASS RATIO VS. AMPLITUDE FACTOR

CHAPTER 4

DESCRIPTION OF TESTS

A circular steel footing 5 7/8" in diameter was designed for this research project. A circular cross-section was chosen to utilize axial symmetry and to utilize existing analytical methods. The dead weight of the footing is 21.7 pounds. Provision was made in the design so that the weight of the footing could be varied. A more complete description of the footing is presented in Chapter 5.

An input force of 1.84 pounds was used in all tests. This force was selected because of the ease with which it could be monitored on a recorder and because of its suitability of the characteristics of the vibration generator. It was also believed that this force was small enough to avoid large non-linear behaviour.

The footing rested upon the surface of a densely compacted Ottawa sand. A bin 54" square and 49" deep was constructed of concrete blocks and lined with styrofoam to avoid wave reflection. The Ottawa sand was compacted to a depth of 31".

Five series of tests were performed in the research program. Each test was conducted at a different weight of footing resulting in different mass ratios. The frequency range of each test was approximately 30 - 150 cps. The weight and mass ratio of each test appears in Table III.

TABLE III

DESCRIPTION OF TEST SERIES

Series No.	Weight of Footing (LBS)	Mass Ratio	Confining Pressure (LB/FT^2)	Shear Modulus (LB/IN^2)	Maximum Amplitude of Vibration ($IN \times 10^{-4}$)	Resonant Frequency (cps)
I	21.7	13.5	58	2209	3.44	99.4
II	29.8	18.5	80	2672	3.32	93.9
III	37.9	23.5	101	3086	3.23	89.8
IV	46.5	28.8	124	3489	3.16	86.4
V	54.6	33.8	145	3842	3.11	83.8

Soil Description

The soil used for this project was a densely compacted uniform Ottawa sand. The water content was found to be negligible. The specific gravity was determined to be 2.66. The density of the sand was found to be 110 lb/ft^3 which corresponds to a void ratio of 0.51. The grain size distribution appears in Figure 6.

Shear Modulus of Soil

Hardin and Richart (1963) have investigated the shear modulus for dry Ottawa sand. They found experimentally that the shear wave velocity was dependent on the confining pressure and the void ratio and independent of grain size and distribution for the range tested which were between the No. 20 and No. 140 standard sieves. The resonant column method was used with a double amplitude of vibration of 10^{-3} radian at the free end with the other end fixed. The experimentally obtained results were presented in the form of empirical equations for determination of the shear wave velocity. The maximum deviation of the experimental results and the empirical equations was about 10 per cent.

$$C_s = (170 - 78.2\ e)\sigma_c^{1/4} \quad \text{for } \sigma_c > 2000\ lb/ft^2 \tag{25}$$

$$C_s = (119 - 56.0\ e)\sigma_c^{3/10} \quad \text{for } \sigma_c \leq 2000\ lb/ft^2 \tag{26}$$

where σ_c = confining pressure in lb/ft^2

C_s = shear wave velocity in ft/sec

e = void ratio

Hardin (1965) converted the above equations to predict the shear modulus. The shear modulus may be expressed as

$$G = \rho C_s^2 \tag{27}$$

where G = shear modulus

Substitution of C_s from equation (27) in equation (26) yields the following results:

$$G = \frac{(32.17 - 14.80\ e)^2}{(1 + e)} \sigma_c^{1/2} \tag{28}$$

for $\sigma_c > 2000$ lb/ft^2

$$G = \frac{(22.52 - 10.60\ e)^2}{(1 + e)} \sigma_c^{3/5} \tag{29}$$

for $\sigma_c \leq 2000$ lb/ft^2

where G = the shear modulus in psi for σ_c in lb/ft^2

The effect of varying the amplitude of vibration on the shear modulus has been investigated by Hall and Richart (1963). They used the resonant column method for Ottawa sand. They found that the shear modulus decreases as the amplitude of vibration increases. This decrease was a maximum of 15% as the double amplitude of vibration was increased from 1×10^{-5} to 2.5×10^{-3} radians.

Determination of the Confining Pressure

The difficulty of determining the shear modulus is the computation of the confining pressure for a foundation resting upon a semi-infinite mass. Chae (1964) assumed the confining pressure to be the static weight divided by the contact area. A check of this assumption can be made using the experimental

resonant frequency and equations (6) and either (28) or (29)

$$a_o = 2\pi f_o r_o \sqrt{\frac{\rho}{G}} \qquad (6)$$

$$G = \frac{(22.52 - 10.60\ e)^2}{(1 + e)}\ \sigma_c^{3/5} \qquad (29)$$

The value of a_o is determined theoretically and the value of f_o is determined experimentally. The value of G can now be calculated from equation (6). Substitution of G into equation (29) enables a calculation of σ_c which can then be compared with the original assumption of calculating σ_c. Using this method, Chae found that the confining pressure was less than the assumed average normal pressure. The confining pressure may be expressed as the following function of the average normal pressure.

$$\sigma_c = \kappa \frac{W}{A_c} \qquad (30)$$

where κ = confining pressure factor

W = weight of foundation

A_c = contact area

Using the above method Chae found that κ was in the range of 0.49 to 0.56 for densely compacted Ottawa sand.

The value of κ was assumed to be 0.50 for this research program. The value of the shear modulus and its associated confining pressure is shown in Table III, and is graphically depicted in Figure 7.

Poisson's Ratio

Phalen (1963) has determined the compressive wave velocity for cohesionless soils using a seismograph with dynamite as a

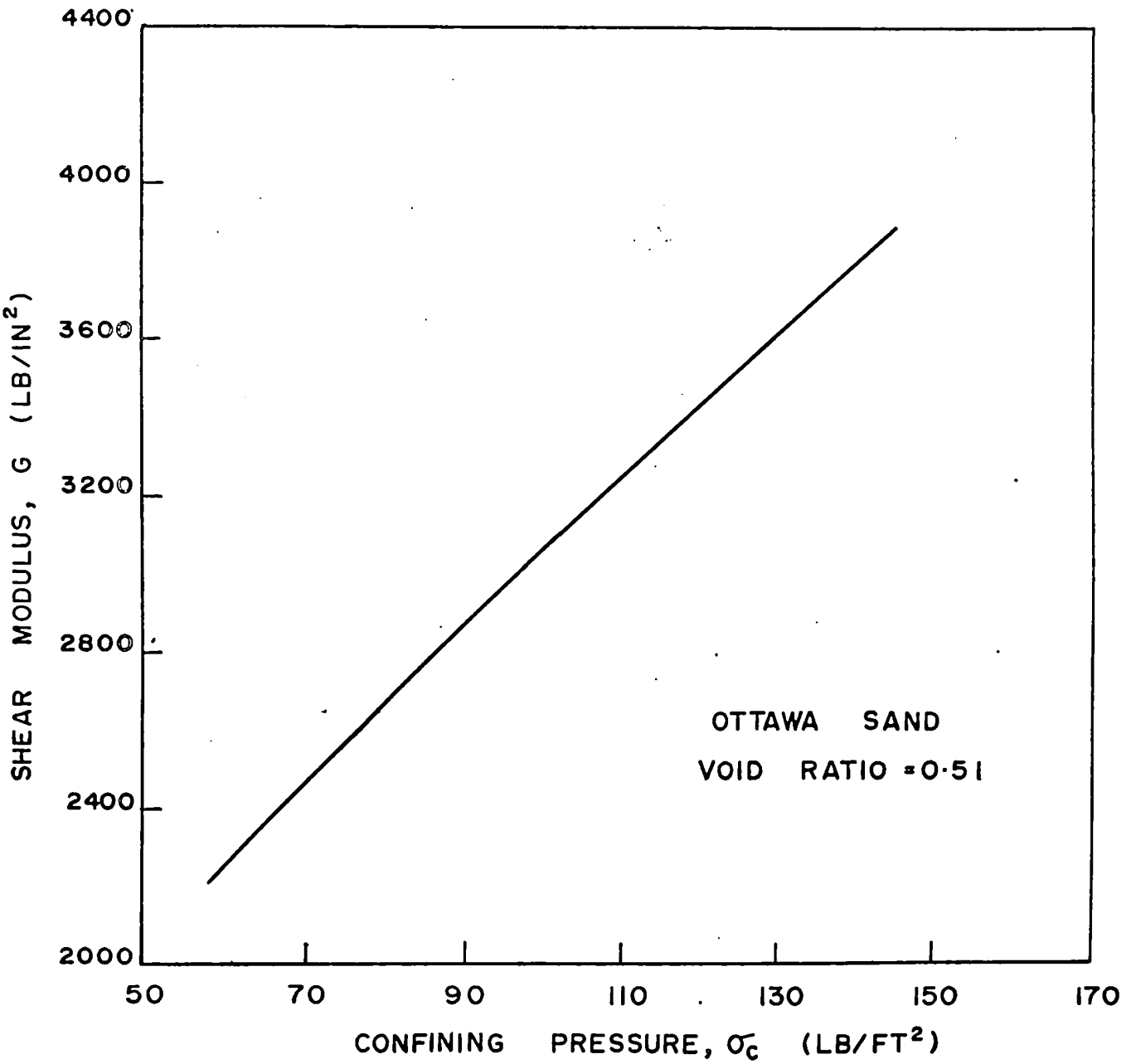

FIG. 7 SHEAR MODULUS VS. CONFINING PRESSURE

source of wave energy. The tests were conducted in-situ and void ratio, density and gradation were determined. Shear wave velocities were computed using data from Hardin and Richart (1963).

Poisson's ratio may be determined by the following equation if the shear and compressive wave velocities are known.

$$\left(\frac{C_s}{C_c}\right)^2 = \frac{1 - 2\nu}{2(1 - \nu)} \tag{31}$$

Using the above equation Phalen determined Poisson's ratio to be in the range of 0.29 - 0.40. Phalen observed that the compressive wave velocity was independent of grain size and distribution and independent of water content to the point of saturation.

Phalen's results are consistent with those published by Leonards (1962). Leonards states, without citing experimental qualification, that for dense sands Poisson's ratio is 0.30 - 0.35.

Whitman (1966) determined Poisson's ratio using data from the U.S. Army Engineer Waterways Experiment Station (1963). The shear and compressive wave velocities were measured to determine Poisson's ratio. For a uniform fine soil, Poisson's ratio was determined to be in the range 0.25 - 0.40.

The determination of the displacement functions have been determined for Poisson's ratio of 0, 1/4, 1/3, and 1/2 (Sung, 1953). For the purposes of this research project, Poisson's ratio was assumed a value of 0.33. This value is consistent

with experimental data and enables theoretical predictions using Sung's theory.

Static Contact Pressure Distribution

Faber (1933) determined experimentally the contact pressure distribution beneath a circular footing resting in the surface of a dry sand. The footing was 12" in diameter and consisted of concentric rings which were attached to a solid upper plate by means of three steel rods 1/4" in diameter. Extensometers were attached to the steel rods to measure their deflection enabling a determination of the average pressure distribution beneath each ring. Faber found that the contact pressure distribution conformed to a parabolic pressure distribution with the pressure at the centre approximately twice the average pressure while the pressure at the edge was negligible. The pressure at the centre, however, became more concentrated as the load increased. Chae (1964) also using a footing consisting of concentric rings obtained results similar to those of Faber.

It was assumed that the static pressure distribution would be parabolic for the rigid footing used in this research program. Assuming further that the parabolic pressure distribution would be true for the dynamic case, the Reissner-Sung theory was used for theoretical predictions of maximum amplitude of vibration and resonant frequency.

Predicted Resonant Frequencies and Maximum Amplitude of Vibration

The Reissner-Sung theory was used to determine the dynamic response of the footing for each series of tests. A parabolic pressure distribution was assumed with Poisson's ratio of 1/3 and the shear modulus values as determined previously. The predicted resonant frequencies and amplitudes of vibration appear in Table III and are shown graphically in Figure 8. A more complete analysis of the predicted dynamic response appears in Chapter 6 along with the experimental results. An IBM 7040 computer was used to predict this response. The computer program appears in Appendix C.

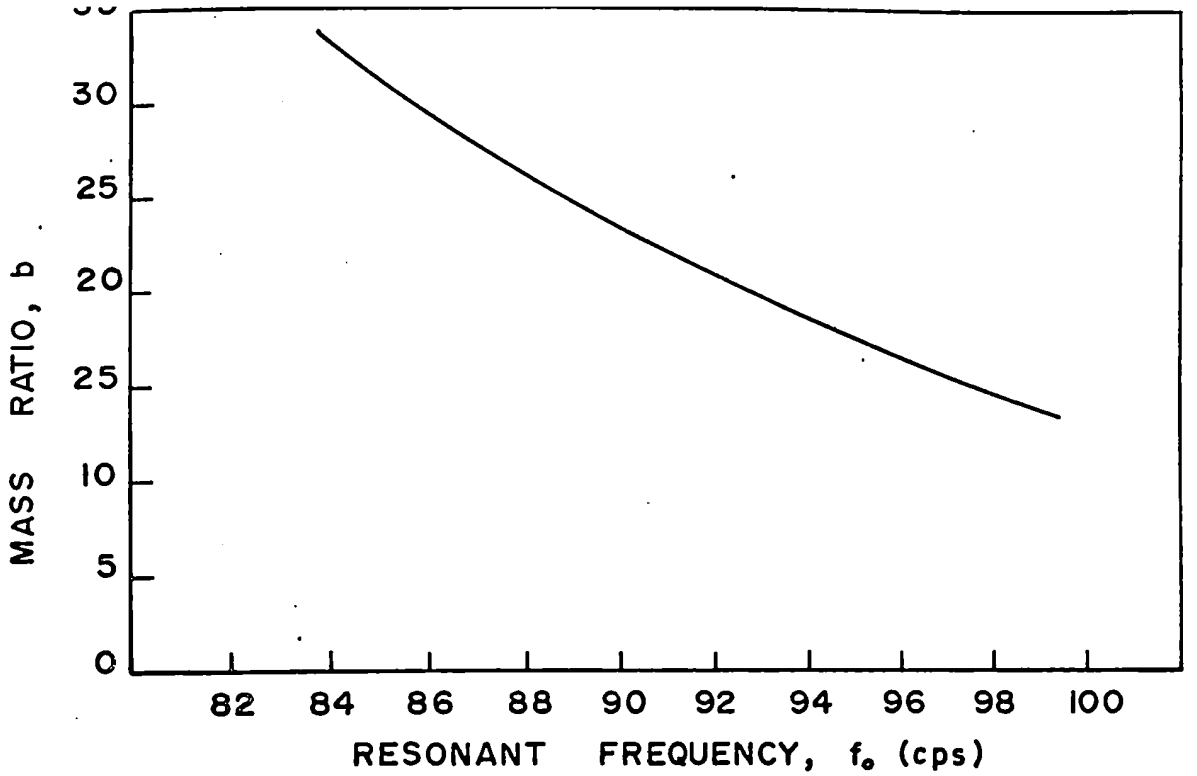

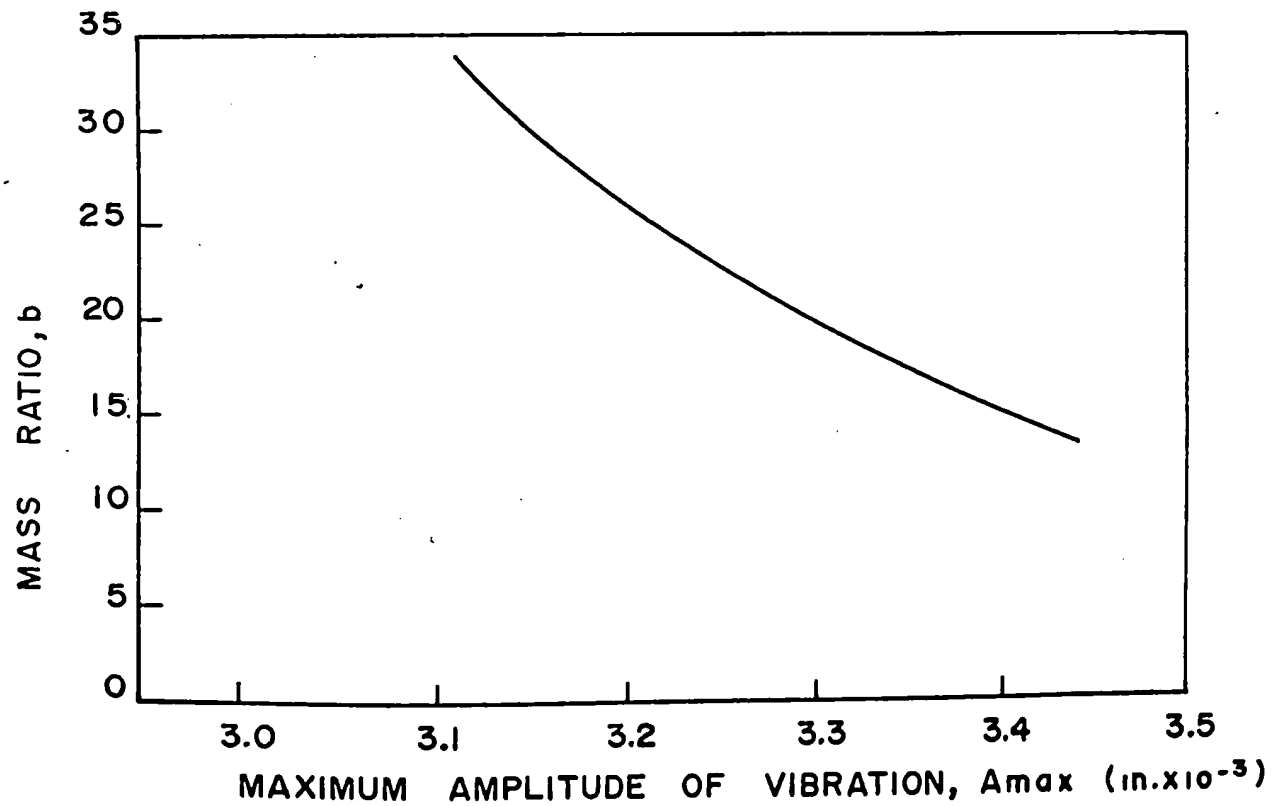

FIG. 8 PREDICTED RESONANT FREQUENCY AND MAXIMUM AMPLITUDE OF VIBRATION VS. MASS RATIO

CHAPTER 5

EXPERIMENTAL APPARATUS AND PROCEDURE

Soil Bin

A soil bin was constructed to contain the soil. The bin was constructed of 16" x 8" concrete blocks held together with mortar. The corners of the bin were vertically reinforced to resist the soil pressure. The inside dimensions of the bin are 54" square and 49" deep. The inside and bottom of the bin is lined with 1" thick styrofoam to minimize wave reflection. Chae (1964) used 1/2" thick Celotex board for the same purpose.

Sand Compaction

The bin was filled with Ottawa sand which was compacted to maximum density to minimize settlement of the footing. The apparatus used to achieve this density was a Syntron Model V-9-B Electric Vibrator. A 12" square steel plate 1/4" thick was secured to the vibrator.

Laboratory tests were performed to determine how the maximum density could be achieved. A small pan of known volume was buried in the sand before vibration was applied. After vibration, the pan was carefully dug out and the sand was levelled to the top of the pan. The weight of the sand was then determined enabling a density determination. By a trial and error process, it was determined that the maximum density was 110 $lb/ft.^3$. It was found that for a 4" layer of sand, one minute of vibration with the rheostat set at 80 would achieve maximum density. Chae (1964) using a similar Ottawa sand also found that the maximum density was 110 $lb/ft.^3$.

Sand in the bin was compacted using the above technique. The weight of sand put in the bin was recorded and the final volume calculated. An average density of 112 lb/ft.^{3} was determined. A density of 110 lb/ft.^{3} was used for the analytical computations since it was believed that the laboratory method was more accurate than the field test.

After the completion of a test the surface of the soil was levelled and vibrated using the previously discussed technique. In addition the surface was again vibrated using a rheostat setting of 50. The purpose of this additional vibration was to compact the uppermost layer of grains. At various stages of the testing program sand was added and removed from the bin for tests other than those reported herein. All tests performed for this research program were conducted with a depth of sand approximately 30 to 31 inches.

Footing Description

The footing consists of a hollow steel cylinder 5 7/8" in diameter and 8" in height. A detailed drawing of the footing appears in Figure 9. The base of the footing was constructed so that eight pressure transducers could be mounted to measure the pressure distribution on the footing-soil interface. The flanges of the pressure transducers were rigidly encased between the cylinder and the lower plate to avoid any movement when pressure is applied. The cylinder and lower plate were cadmium coated to avoid rusting. The diaphragms of the transducers protruded the lower plate by

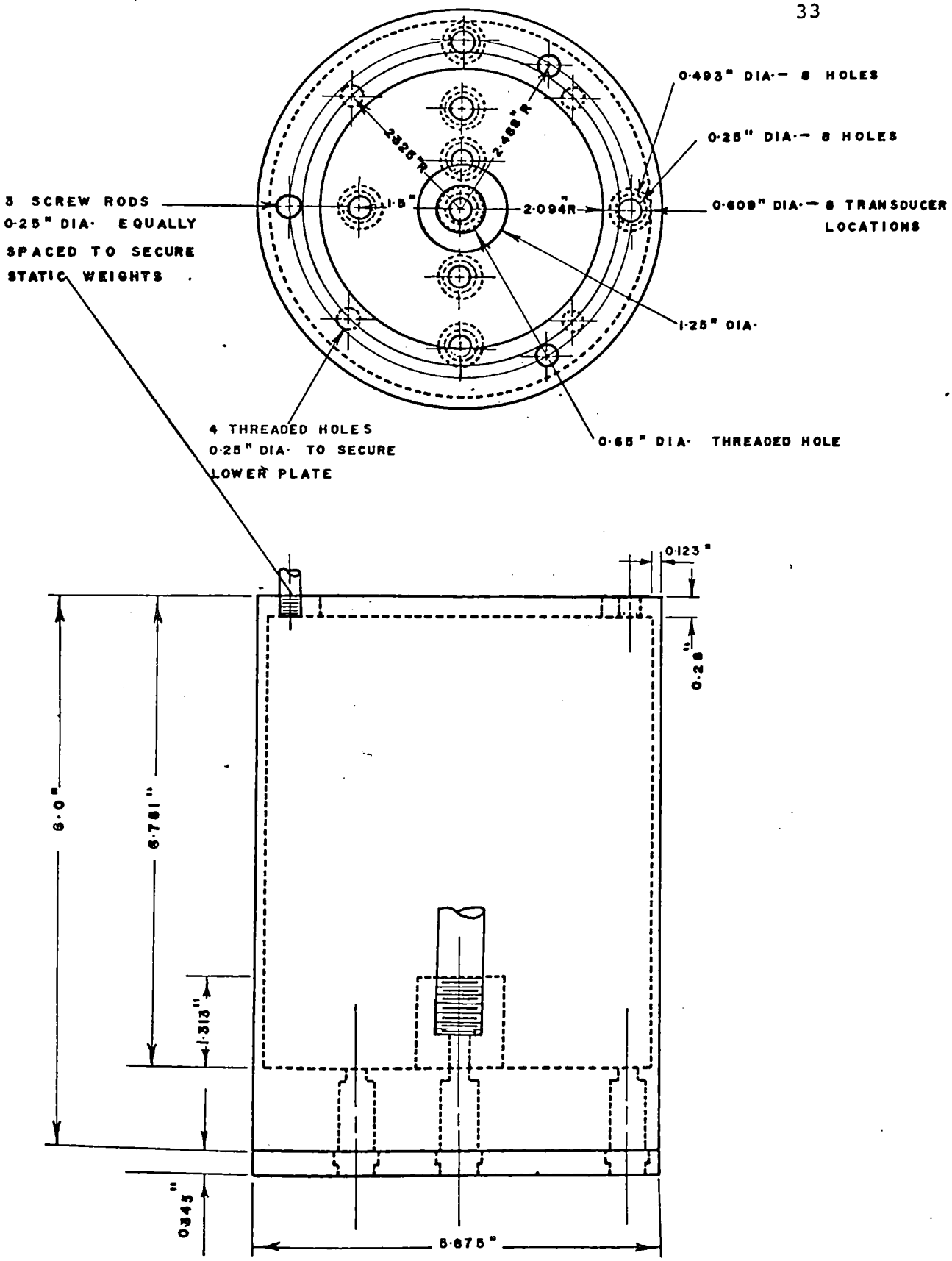

SCALE: 1" = 2"

FIG·9 DETAILS OF RIGID FOOTING

0.005".

A diagram describing the location of the eight transducers appears in Figure 10. Transducers 1 and 8, and 2 and 7 were located at the same radial distance respectively. These transducers allow a check of symmetrical loading conditions.

A 3/4" steel shaft is secured to the base of the cylinder to apply vibrational forces to the footing. Three 1/4" screw rods are attached to the top of the footing to secure static weights. The static weights consist of 12" diameter steel discs of varying weights.

Frame and Loading Apparatus

Two rectangular frames constructed of channels and measuring 6' x 4' were positioned at each end of the sand bin. A general view of the frame, soil bin and electronic equipment is shown in Plate I. Three sides of the frame are constructed of 8[11.5 channel with the remaining side of 10[15.3 channel. The larger channel was anchored to the wall and one side was anchored to the floor.

Two 14 WF 30 beams 8' long were bolted to the frames such that their webs were 2' apart. Mounted vertically at the centre of each beam is a 22" section of 10[15.3 channel. Each section of channel has two 1/2" vertical slots 3" apart and 20" long. A 17" section of 14 WF 30 beam is mounted between these channels and can be positioned vertically within the limits of the slots. A vertical control device

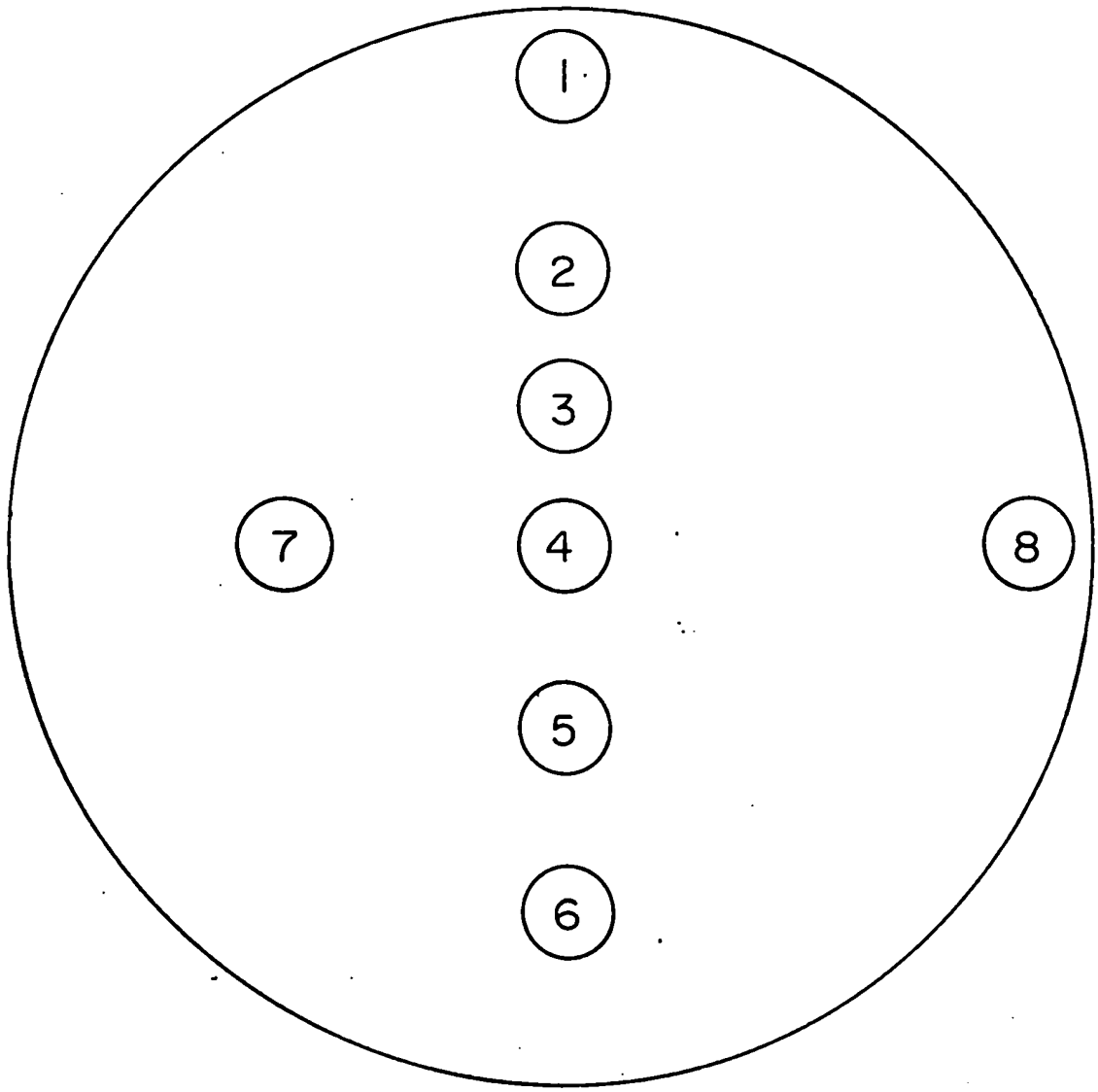

FULL SCALE

TRANSDUCER NO.	LOCATION	TRANSDUCER NO.	LOCATION
1	$2\frac{9}{16}$"	5	1"
2	$1\frac{1}{2}$"	6	2"
3	$\frac{3}{4}$"	7	$1\frac{1}{2}$"
4	0"	8	$2\frac{9}{16}$"

FIG.10 PRESSURE TRANSDUCER LOCATIONS

PLATE I OVERALL APPARATUS

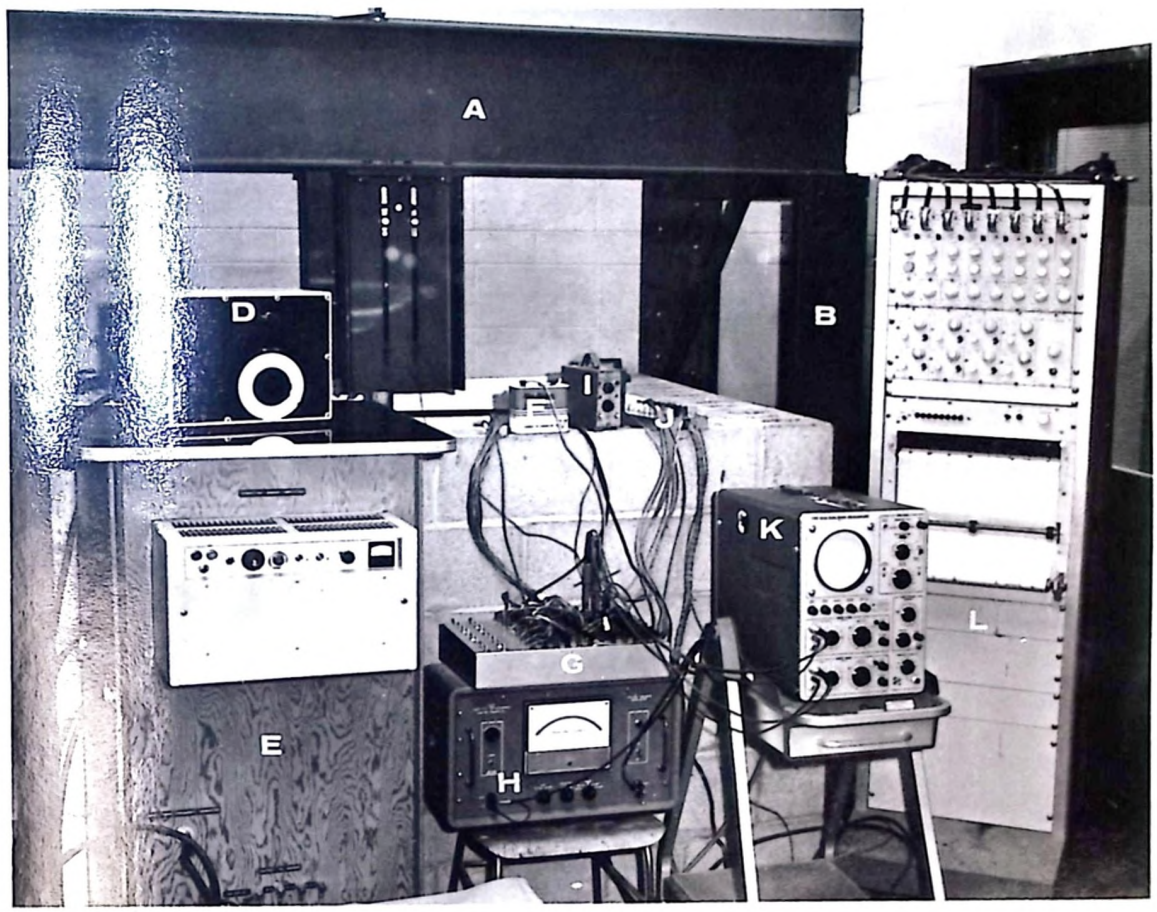

A- BEAMS
B- FRAME
C- SOIL BIN
D- FREQUENCY GENERATOR
E- POWER AMPLIFIER
F- DRY CELL
G- SWITCHING BOX
H- PHASE METER
I- CHARGE AMPLIFIER
J- COUPLING BOX
K- OSCILLOSCOPE
L- RECORDER

PLATE II FOOTING LOADING SYSTEM

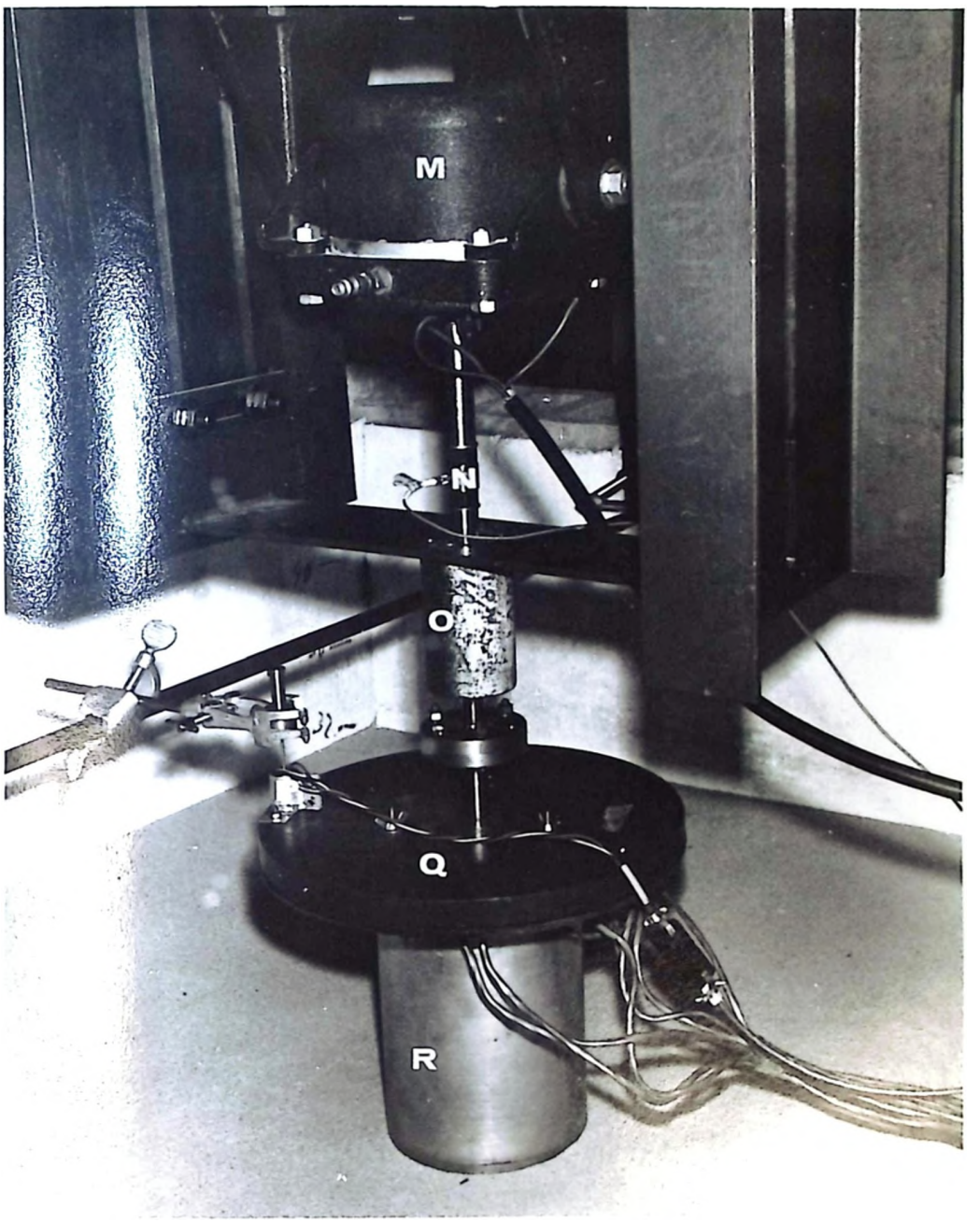

M- VIBRATION GENERATOR
N- FORCE LINK
O- CYLINDER CONTAINING BALL BUSHINGS

P- DISPLACEMENT TRANSDUCER
Q- WEIGHTS
R- FOOTING

output on a recorder. The calibration factors were found to be linear within the range of 0 - 25 lb/in^2 for every transducer.

(b) Force Link and Charge Amplifier

A Kistler Model 932A quartz force link was used to measure the dynamic force. The force link was connected between two lengths of shaft as shown in Plate II. Loads to 4000 pounds compression and 2000 pounds tension can be measured in temperature environments from -320°F to 500°F. The response time is 20 microseconds and has a natural frequency of 54,000 cps. It has a flat dynamic response to 5000 cps.

A Kistler Model 503 Universal Dial Calibration Charge Amplifier was used in conjunction with the force link. The charge amplifier is designed to convert charge signals from the piezoelectric force link to a voltage output which can be displayed on indicating or recording equipment. The charge amplifier has a flat frequency response from 10 to 1000 cps with an ambient operating temperature of 30° to 150°F.

The force link-charge amplifier system was calibrated by applying a known load to the force link. The output signal was monitored on the recorder. The calibration factor was found to be linear to 300 pounds.

(c) Displacement Transducer

A Sanborn Model 7DCDT-050 Differential Transformer Displacement Transducer having a full scale stroke of ±0.05" was used to measure the amplitude of vibration. The design

of the transducer inherently eliminates phase shift connection. It has an ambient temperature range of -65° to 140°F. The input to the transducer was supplied by a 6 volt dry cell. The transducer was calibrated using a known displacement and monitoring the output on the Beckman recorder. The calibration factor was linear within the full scale stroke.

The displacement transducer is composed of a cylindrical core and an armature. The armature fits inside the core and relative movement between the two results in a displacement reading. The core was attached to either the footing or the weights by means of a casing. A screw and nut assembly was devised to control the movement of the armature. This apparatus was found to be necessary to position the armature within the full stroke distance of the null position. The armature was held in position by a clamp attached to a 5/8" diameter steel rod which was secured at each end of the soil bin. The displacement transducer assembly is shown in Plate II.

(d) Vibration Generator

A Goodman Model 790 Vibration Generator was used to exert the vibrational force. The vibration generator has a frequency range from 10 to 500 cps with a peak force of 25 pounds and has a resonant frequency of approximately 15 cps. The vibration generator has a total permissible stroke of 0.5". The amplitude of vibration encountered during testing were in the order of 10^{-4} inch so that the stroke limitation did not present a restriction. Settlement, however, did occur in the order of 1/3" to 1/2" but this was counteracted by lowering of the vibration generator through the use of the vertical control

device.

The operation of the vibration generator is controlled by a frequency generator. The signal from the frequency generator feeds the power amplifier which in turn feeds the vibration generator. The vibrational force was found to decrease with increasing frequency for a given amplitude setting on the frequency generator. Since a constant force was desired throughout the testing procedure, it was required to adjust the amplitude setting as the frequency was varied.

(e) Oscilloscope and Phase Meter

To measure phase differences an Ad-Yu Type 405H Precision Phase Meter was used. This instrument indicates phase differences directly in degrees. It has a frequency range of 8 to 250,000 cps. The accuracy is 1° or 2% up to 200,000 cps. The phase reading is not affected by fluctuation of signal amplitudes in either one or both input channels within its frequency range.

The input signal to each channel must be within the range of 2 to 30 volts. The output vertical amplifier of a Tektronix Type 502A Oscilloscope was used to feed the phase meter. The amplifier provides a vertical signal output of approximately 2 volts per centimeter of deflection. This amplification was found to be sufficient for activation of the phase meter. The oscilloscope was also used to display visually the wave forms.

(f) Recorder

A Beckman-Offner Type R Dynograph was used to record output signals. The basic modules which are used in the instrument are couplers, preamplifiers, power amplifiers, writing elements, paper drives and power supplies. The recorder has eight separate channels that may be used simultaneously. The output is recorded on paper using ink pens. The recorder can supply if necessary the excitation voltage to transducers or other electronic equipment.

Description of Electronic System

The output signals of eight pressure transducers, the force link, and the displacement transducer needed to be recorded. Since the recorder is capable of recording simultaneously only eight signals, only six pressure transducers were used. The output of the check transducers were not recorded except for static tests. Static pressure distribution tests being performed concurrently and which will be reported separately indicated good agreement between check transducers. It was assumed that this agreement would hold for the dynamic situation.

The recorder was used to measure the amplitudes of the various transducers. Phase differences were measured on the phase meter. To accelerate the recording procedure a switching box was constructed which could switch the output from the recorder to the oscilloscope and phase meter system. It was found that electrical interference occurred with the

pressure transducers during phase angle measurements. The interference was eliminated by using a 6 volt dry cell to excite the pressure transducers rather than the excitation supplied by the recorder.

A flow chart of the electronic system is shown in Figure 11. The frequency generator controls the frequency and force of the vibration generator by the power amplifier. The vibration generator activates the pressure transducers, force link, and displacement transducer. The input to the pressure transducers is supplied by the recorder when measuring amplitudes and by a dry cell when measuring phase angles. The charge amplifier changes the output of the force link to voltage. No excitation is required for the force link. The input to the displacement transducer is supplied by a 6 volt dry cell. The output of the pressure transducers, force link and displacement transducers are fed into a switching box. From the switching box the outputs can be fed to either the recorder or the phase meter. The recorder is connected to the switching box through a coupling box. The oscilloscope amplifies the output from the switching box to the phase meter.

Testing Procedure

1. The sand surface was levelled and compacted before testing was started.

2. The weight of the foundation was selected and the appropriate weights were added and secured to the footing

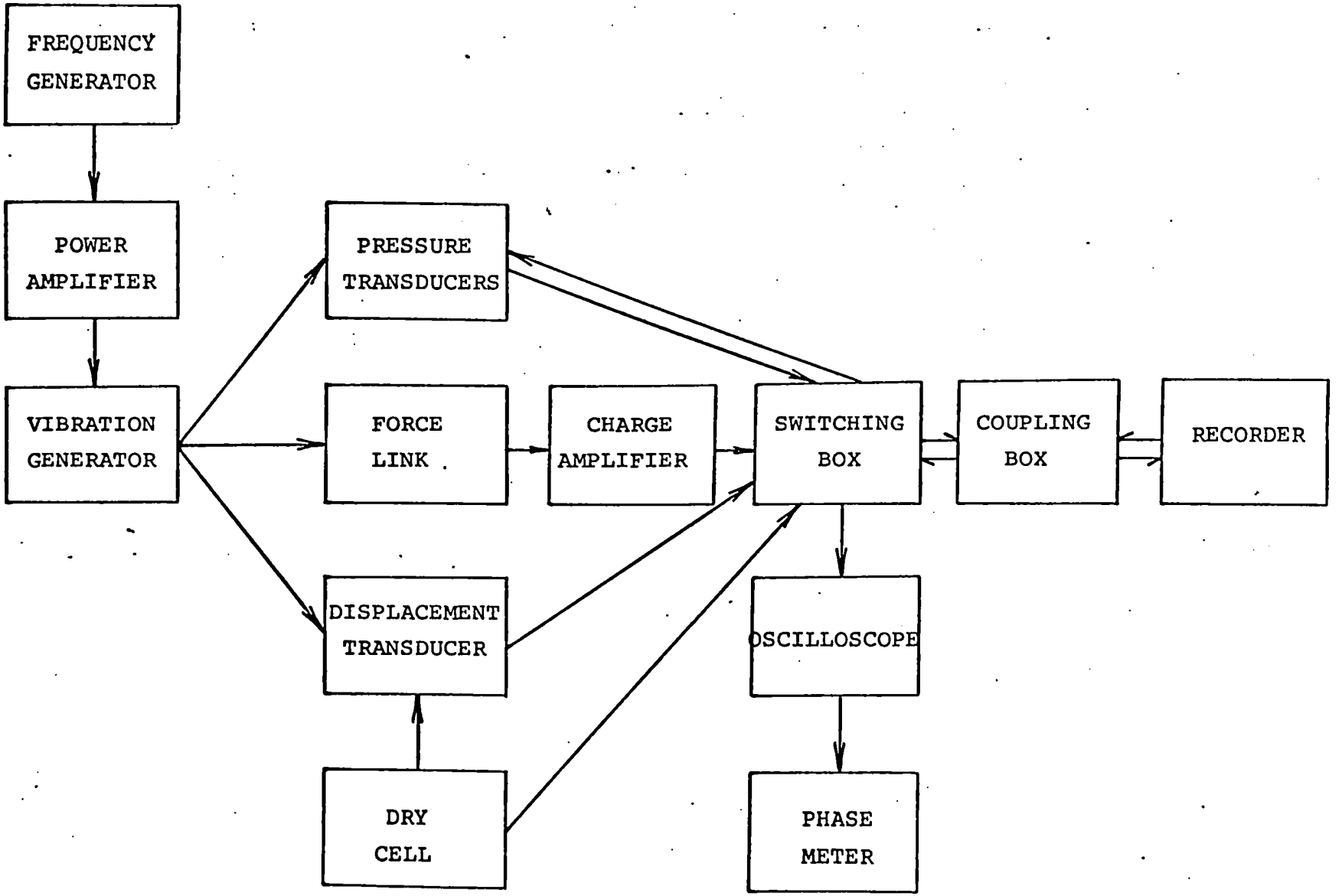

FIG. 11 FLOW CHART OF ELECTRONIC SYSTEM

as necessary.

3. The footing was placed upon a piece of plywood measuring 8" x 8" x 1/4" which rested on the sand. The purpose of this was to minimize sand disturbance during assemblage of the apparatus. The footing was attached to the vibration generator by a shaft. The cylinder containing the shaft was aligned vertically using a transit. Realignment was not necessary provided the cylinder was not moved. The footing was lifted up and the piece of plywood gently removed. The footing was then placed on the soil and the loading apparatus bolted rigid.

4. Static pressure distribution tests were performed before each dynamic test. The footing was vibrated for about a minute to ensure that the footing came into full contact with the soil. The vibration was then stopped and the pressure readings recorded. The process was repeated until about five sets of readings were recorded. Before the dynamic test was commenced, the pressure transducers were adjusted to zero output.

5. The displacement transducer was then positioned and adjusted for a zero output. During the course of the testing the displacement transducer would have to be adjusted a number of times due to settlement of the footing. If settlement greater than approximately 1/4" occurred, the loading apparatus was lowered so that the vibration generator would function properly.

6. For a given frequency the input force was adjusted to 1.84 pounds.

7. The pressure transducers, force link and displacement transducer were monitored simultaneously on the recorder.

8. The phase angle measurements were then recorded. This required switching the outputs from the recorder to the phase meter. Seven phase angles were measured with respect to the input force; they were the six pressure transducers and the displacement transducers.

The force output was fed into the upper beam of the oscilloscope. Phase differences with respect to the input force were measured by plugging the probes of the lower beam to the desired terminals of the switching box. This operation required moving the probes of the lower beam seven times for any given frequency.

9. Procedures 7 and 8 were repeated for each different frequency desired. The range of frequency was approximately 30 to 150 cps. The time of vibration was minimized whenever possible. Vibration was applied only when readings were to be recorded. This procedure was necessary to minimize settlement and prevent overheating of the vibration generator which occurred generally at frequencies greater than 100 cps.

10. Each test was conducted at least twice to check the reliability of the results being obtained. Tests for Series I were conducted eight times; the last three tests, however, were the only ones performed with the instrumentation as described herein.

Problems Encountered in Experimental Procedure

There were two major difficulties encountered in the experimental program. For proper operation of the displacement transducer, there must be no friction between the armature and core. The clearance between them is small and this resulted in a tedious task of adjustment. Further adjustment was also needed as the footing settled to ensure that the armature did not fall out of the full stroke range. Replacement of the displacement transducer by an accelerometer was considered but had to be abandoned since no accelerometer in the low acceleration range was readily available.

The second major difficulty encountered was the measurement of phase differences between the input force and the pressures. The phase meter can measure phase differences within 2% but this is dependent upon a steady symmetrical wave input. Fluctuation of a phase difference could be seen by movement of the phase meter needle. Fluctuation was due mainly to poor waveform from the pressure transducers. The reason for this was the low output of the pressure transducers, that is, less than 1 lb/in^2 where the range of the transducers is 0 - 25 lb/in^2 and 0 - 100 lb/in^2. The higher range transducers generally gave the least accurate pressure amplitudes and phase differences. The accuracy increased as the pressure amplitudes increased and gave the best results at the resonant frequency of the footing-soil system.

CHAPTER 6

RESULTS AND DISCUSSION

Amplitude of Vibration

The amplitude of vibration as a function of frequency for a mass ratio of 13.5 is presented in Figure 12 for both the footing and frame. The vibration of the frame was measured with the displacement transducer mounted to the centre of the beam which supported the vibration generator. The amplitude of vibration of the footing was first measured and then the test was repeated measuring the amplitude of vibration of the frame. The test with b = 13.5 was the only test conducted in which frame vibration was measured.

The footing vibration indicates four peaks at frequencies of 24, 34, 51 and 90 cps while the frame has peaks at 24, 34, 51 and 97 cps. The first three peaks are attributed to resonant frequencies of the frame. Since the frame vibration test shows no peak at 90 cps, the resonant frequency of the footing-soil system is 90 cps. The influence of the resonant frequency of the frame at 97 cps is shown by the non-symmetrical shape of the footing response curve in the range of 96 - 120 cps.

The results of the frame vibration test show that no amplitude of vibration occurs in the range of 60 - 90 cps. The resonant frequencies for the test series decreased from 90 cps to 81 cps as the mass ratio increased to 33.8. Thus the resonant frequencies of the footing-soil system occurred in a range free of resonant frequencies of the frame. The results shown in Figure 12 occurred under the most adverse conditions

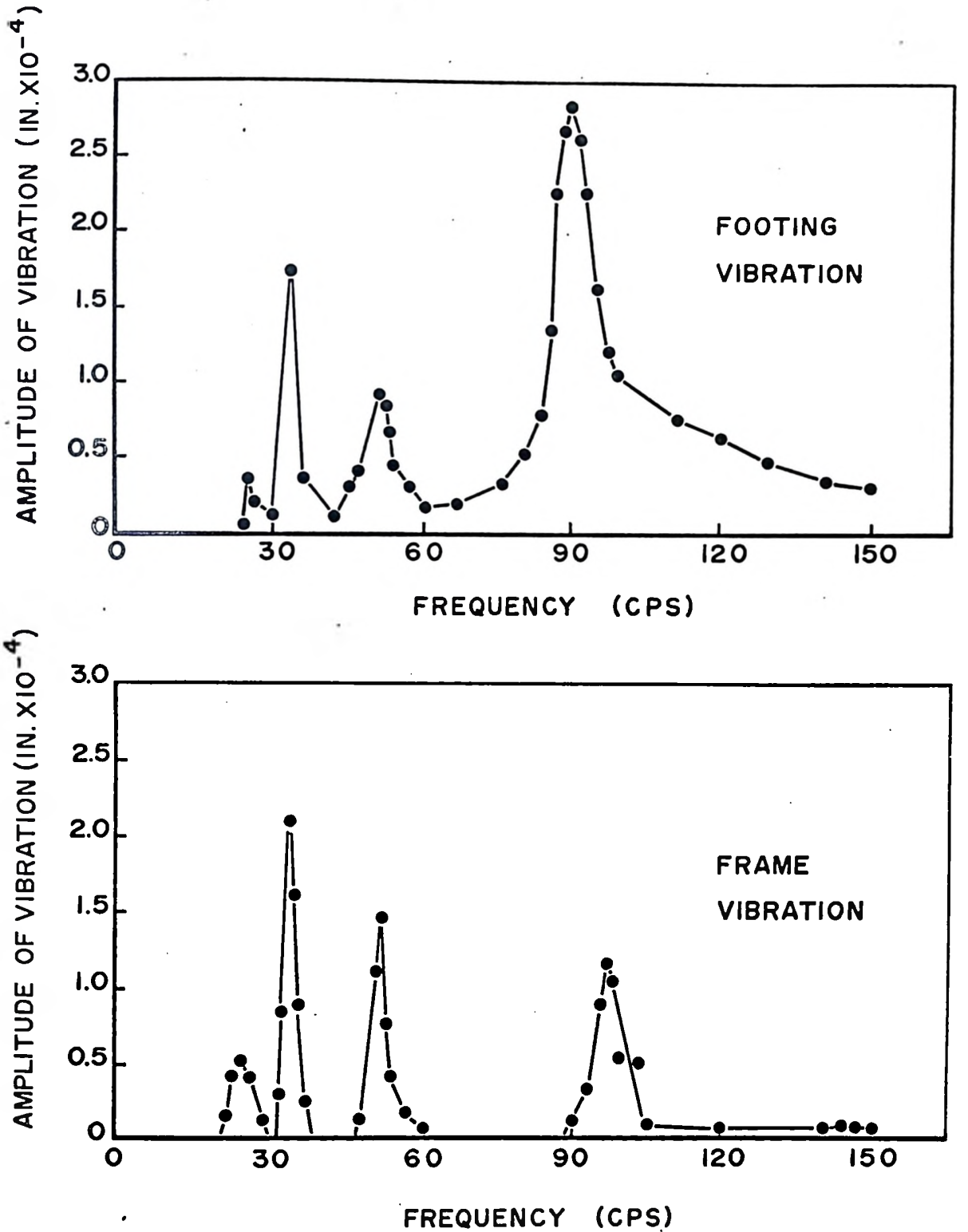

FIG.12 COMPARISON OF FOUNDATION AND FRAME AMPLITUDES OF VIBRATION VS. FREQUENCY FOR b = 13.5

since the resonant frequency of the footing-soil system was closest to a resonant frequency of the frame.

The results of Series IV are used throughout this chapter as a representative sample of the five series. The predicted results refer to those obtained by the Reissner-Sung theory assuming a parabolic pressure distribution with a Poisson ratio of 1/3 unless otherwise specified.

Figure 13 shows both the experimental and predicted amplitude of vibration versus frequency for a mass ratio of 28.8 (Series IV). The experimental results are less than that predicted except for the high frequency range of 130 to 150 cps where the agreement is close. The resonant frequency of the system is 83 cps compared to a predicted value of 86 cps. Amplitudes of vibration due to frame vibration do not appear in Figure 13. This omission was necessary for calculation of the displacement functions which is disccussed later in this chapter.

Phase Angles

Seven different phase angles were measured experimentally. They were the phase difference between the input force and displacement, and the phase differences between the input force and each pressure transducer. Table IV shows the phase angle-frequency relations measured for the test with a mass ratio of 28.8. Each phase angle is shown with an error value. This error is the fluctuation of the phase meter needle. No readings are shown when fluctuation of the needle was five degrees or more. There is a general trend for the phase

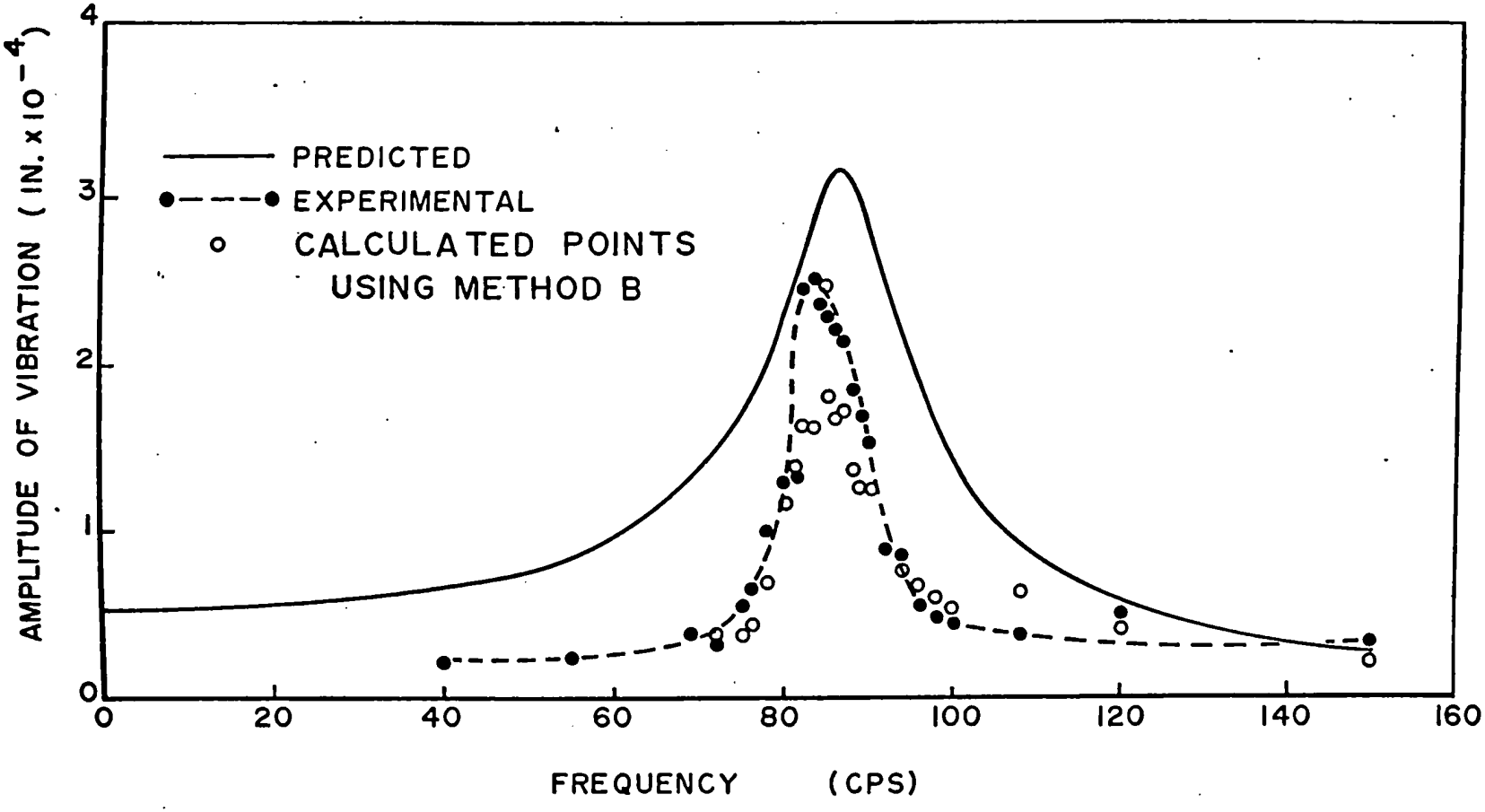

FIG. 13 AMPLITUDE OF VIBRATION VS. FREQUENCY FOR b = 28.8

TABLE IV

PHASE ANGLE - FREQUENCY RELATIONS FOR b = 28.8

FREQUENCY	ϕ_{Q-x}	ϕ_{Q-R_1}	ϕ_{Q-R_2}	ϕ_{Q-R_3}	ϕ_{Q-R_4}	ϕ_{Q-R_5}	ϕ_{Q-R_6}
40 cps	10°±2°	——	15°±3°	8° ±2°	12°±2°	13°±3°	——
55	19 ±1	18 ±2	10 ±1	18 ±2	22 ±2	20 ±2	——
68	21 ±1	24 ±1	17 ±1	22 ±2	25 ±3	28 ±3	——
72	29 ±1	31 ±1	28 ±2	30 ±1	32 ±2	27 ±1	——
75	30 ±1	30 ±1	29 ±2	33 ±1	32 ±2	28 ±1	——
76	35 ±1	33 ±1	30 ±2	33 ±1	32 ±2	33 ±1	——
80	48 ±1	39 ±1	27 ±1	34 ±1	32 ±1	36 ±1	37 ±1
82	85 ±1	86 ±1	75 ±1	73 ±1	68 ±1	69 ±1	69 ±1
83	99 ±1	87 ±1	78 ±1	80 ±1	76 ±1	77 ±1	80 ±1
84	115 ±1	106 ±1	81 ±1	88 ±1	88 ±1	91 ±1	98 ±1
85	112 ±1	112 ±3	104 ±1	110 ±1	108 ±2	114 ±1	118 ±1
86	139 ±1	124 ±1	127 ±1	120 ±1	118 ±1	125 ±1	127 ±2
87	153 ±1	131 ±1	125 ±1	127 ±1	124 ±1	133 ±1	136 ±2
88	149 ±1	135 ±1	132 ±1	126 ±1	127 ±1	130 ±1	138 ±1
89	164 ±1	155 ±1	141 ±1	141 ±1	136 ±1	135 ±1	133 ±1
90	176 ±1	158 ±1	148 ±1	149 ±1	144 ±1	142 ±1	138 ±1
92	162 ±1	159 ±1	145 ±1	151 ±1	146 ±1	143 ±2	140 ±3
94	148 ±1	147 ±1	137 ±1	143 ±1	141 ±1	138 ±3	130 ±4
96	142 ±1	144 ±1	133 ±1	138 ±1	134 ±1	117 ±3	——
98	138 ±1	134 ±1	126 ±1	130 ±2	126 ±1	——	——
100	128 ±1	116 ±1	111 ±1	112 ±3	108 ±2	——	——
108	116 ±1	93 ±1	98 ±1	105 ±1	107 ±1	108 ±2	——
120	174 ±1	174 ±1	171 ±1	166 ±1	170 ±3	165 ±2	——
150	177 ±1	173 ±1	170 ±2	169 ±1	——	——	——

angles to increase as the frequency increases to 90 cps and then decrease to 108 cps and then increase again as the frequency increases to 150 cps. The decrease is attributed to the resonant frequency of the frame at 97 cps. The influence of other frame resonant frequencies is excluded from this table.

The predicted and experimental relation of the phase angle ϕ_{Q-x} and frequency is shown in Figure 14. Both curves exhibit the same general trend but the experimental curve is shifted to the left of the predicted curve. This is to be expected since the experimental resonant frequency is less than the predicted value. The influence of frame resonant frequencies is not shown on this graph.

On the basis of the data shown in Table IV the phase angle ϕ_{Q-R} is a constant across the footing. Differences are attributed to random error. An experimental investigation conducted by Chae (1964) revealed that the phase angle ϕ_{Q-R} was not a constant across the footing. The difference is attributed to footing rigidity. The footing used in this investigation is considered rigid compared to Chae's more flexible footing consisting of concentric rings. A more detailed discussion of the phase angle ϕ_{Q-R} is reported by Ho and Burwash (1968).

Figure 15 shows the experimental and predicted values of the phase angle ϕ_{Q-R} versus frequency. The experimental values were determined by an average of the most accurate readings. Both the experimental and predicted curves

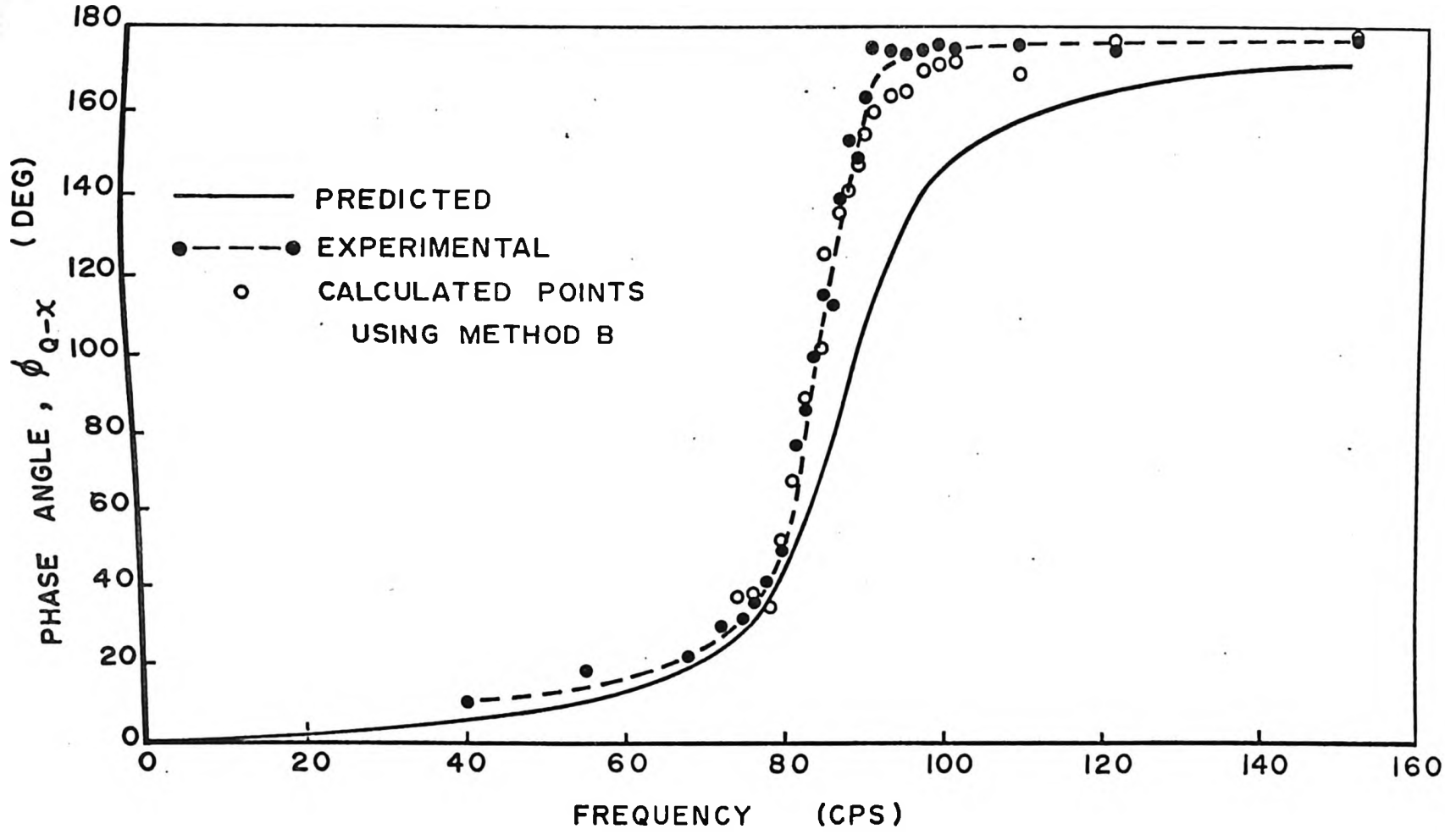

FIG. 14 PHASE ANGLE ϕ_{Q-X} VS. FREQUENCY FOR b = 28.8

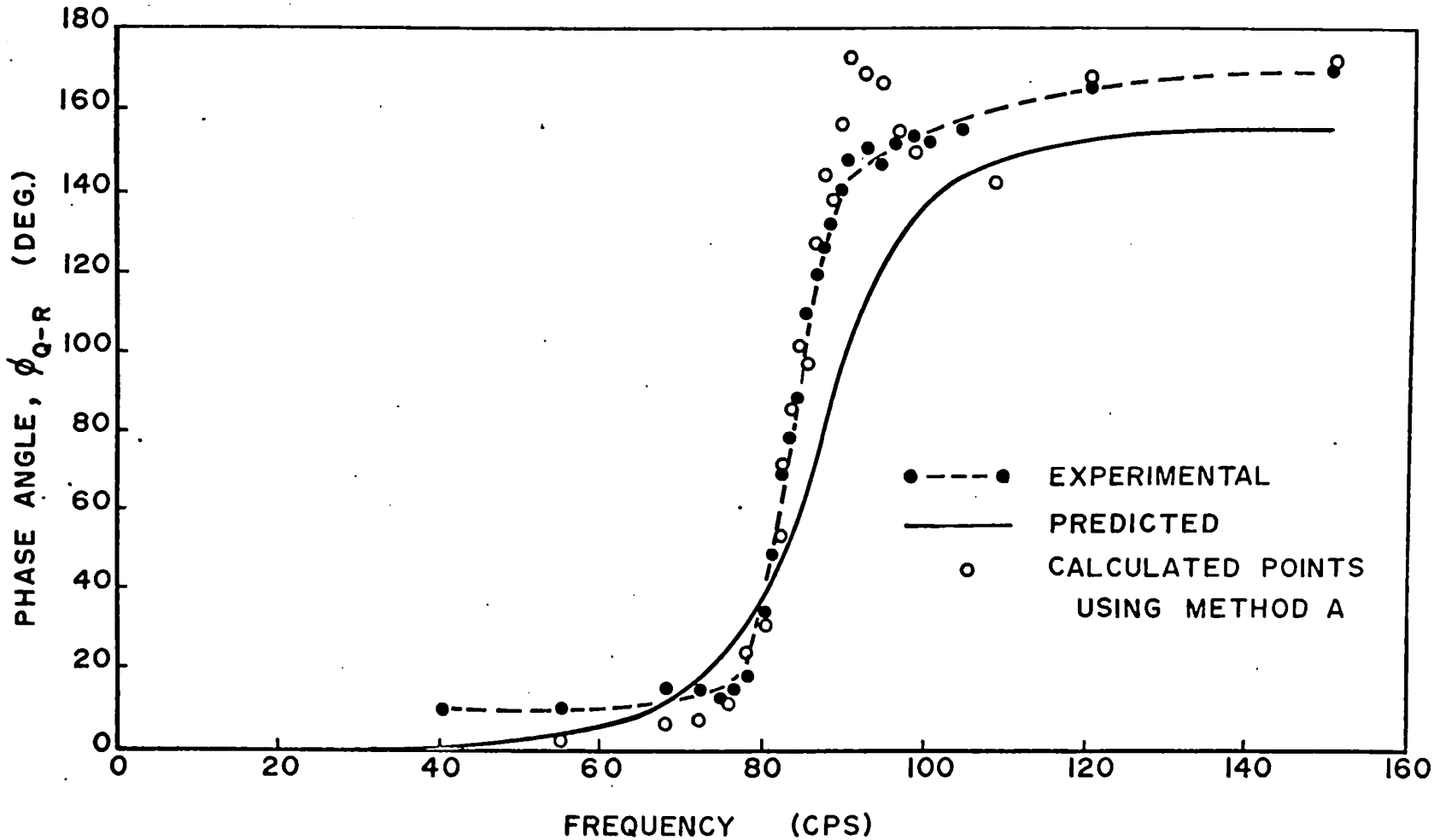

FIG. 15 PHASE ANGLE ϕ_{Q-R} VS. FREQUENCY FOR b = 28.8

exhibit the same trend. The experimental curve is shifted to the left similar to that for the phase angle ϕ_{Q-x}.

Static Pressure Distribution

Static pressure tests were performed to determine the pressure distribution on the footing-soil interface. The results of two such tests are shown in Figure 16. The load was computed by numerical integration of the pressure distribution and agreed within 20 per cent of the applied load. The general trend is a maximum pressure at the centre and a minimum pressure at the edge of the footing. Between these two limits there exists a point of intermediate minimum pressure at the one inch radius. The pressure at the edge of a footing resting on the surface of a cohesionless soil must be zero since the soil has no shear strength at this point.

A more complete investigation of static pressure distribution has been performed with the same footing and will be reported by Ho, Lopes and Burwash (1968). The results of these tests showed a similar pressure distribution to that shown in Figure 16. Two pressure transducers were used to measure the pressure at the one inch radius. The two transducers showed a good correlation of results.

Dynamic Pressure Distribution

Figure 17 shows the dynamic pressure distribution for a mass ratio of 28.8 over a range of five different frequencies. The results for frequencies up to 83 cps show the same general trend as the static tests. The maximum pressure occurs at the centre and the minimum pressure at the edge. The intermediate

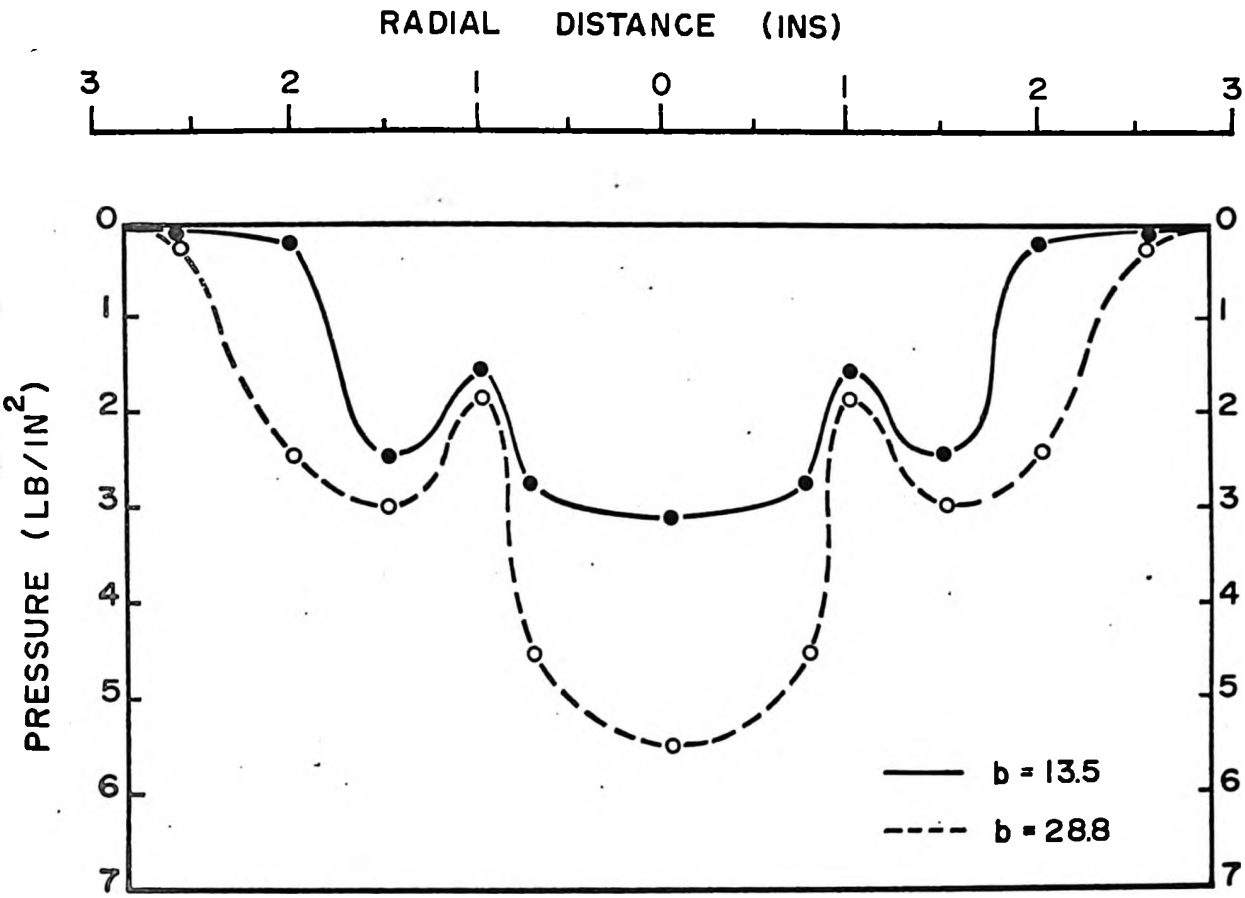

FIG.16 STATIC PRESSURE DISTRIBUTION

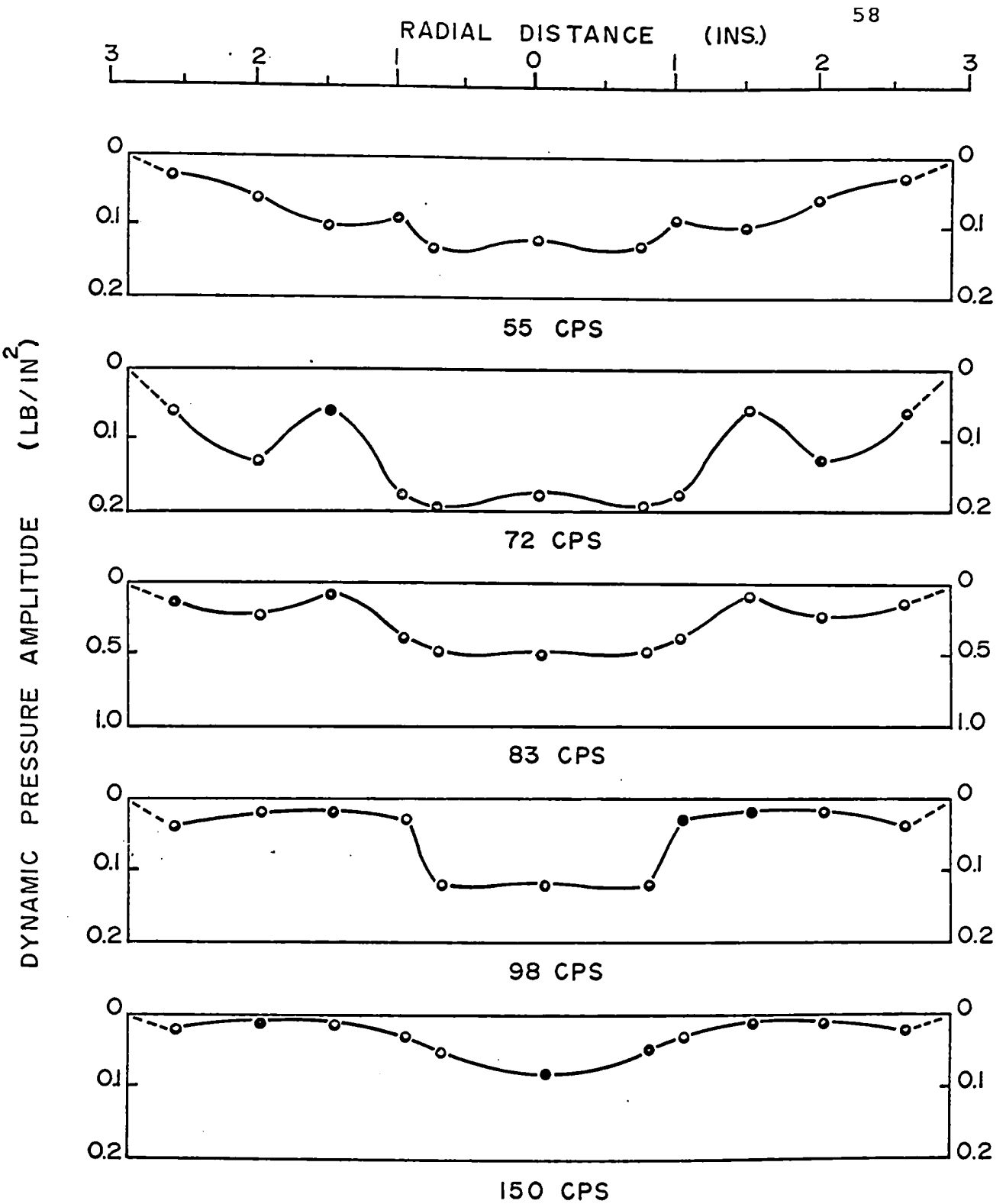

FIG.17 DYNAMIC PRESSURE DISTRIBUTION AT DIFFERENT FREQUENCIES FOR b = 28.8

minimum pressure occurs at the one inch radius at 55 cps and at the 1 1/2 inch radius at 72 and 83 cps. At higher frequencies, however, the intermediate minimum pressure is no longer evident. As the frequency increases to the resonant frequency of 83 cps, the dynamic pressure amplitude increases and then decreases as the frequency increases past the resonant frequency.

The dynamic pressure distribution at the resonant frequency for each mass ratio used in the testing program appears in Figure 18. The same general trend of pressure distribution occurs. The dynamic pressure amplitude increases as the mass ratio increases.

Dynamic Soil Reaction

The experimental and predicted soil reaction as a function of frequency is shown in Figure 19. The soil reaction was calculated by numerical integration of the pressure amplitudes on the footing-soil interface. The soil reaction reaches a maximum value at the resonant frequency. At zero frequency the soil reaction is equal to the input force amplitude Q_1 which is 1.84 pounds. Both the experimental and predicted curves have the same general trend. The magnitude of the experimental soil reaction is less than that predicted and is shifted to the left.

Determination of the Displacement Functions

It was desired to determine the displacement functions from the experimental data. If the displacement functions

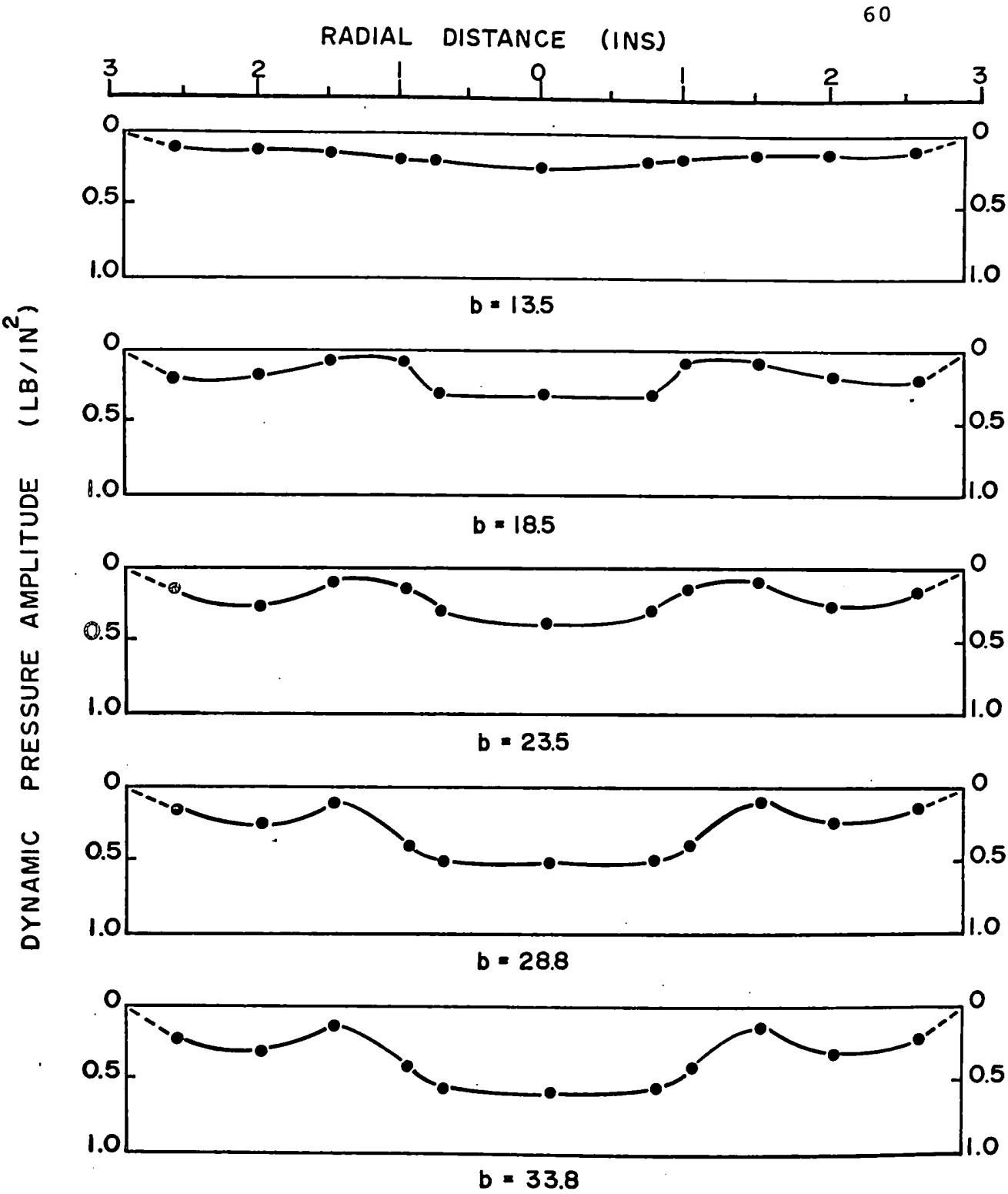

FIG.18 DYNAMIC PRESSURE DISTRIBUTION AT RESONANT FREQUENCY FOR DIFFERENT MASS RATIOS

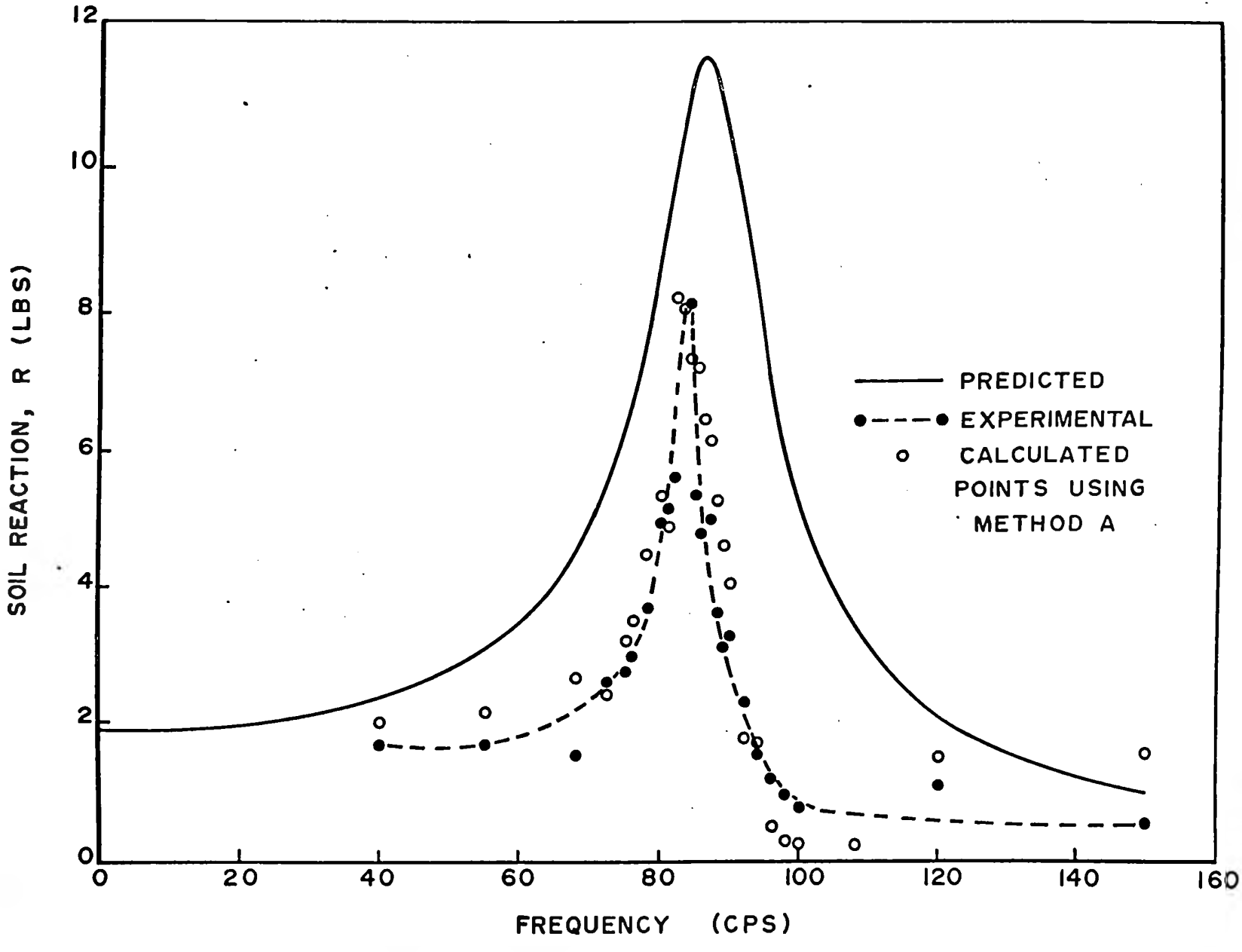

FIG.19 SOIL REACTION VS. FREQUENCY FOR b = 28.8

are known then the response of a foundation of any mass ratio can be determined. Four variables were measured experimentally; they were ϕ_{Q-R}, R_1, X, and ϕ_{Q-x}. Any two of these variables may be used to determine the displacement functions by using the two corresponding equations from the following four equations.

$$\tan \phi_{Q-R} = \frac{ba_o^2 f_2}{1 + ba_o^2 f_1} \tag{11}$$

$$R_1 = \frac{Q_1}{\sqrt{(1 + ba_o^2 f_1)^2 + (ba_o^2 f_2)^2}} \tag{12}$$

$$X = \frac{Q_1}{r_o G} \sqrt{\frac{f_1^2 + f_2^2}{(1 + ba_o^2 f_1)^2 + (ba_o^2 f_2)^2}} \tag{15}$$

$$\tan \phi_{Q-x} = \frac{-f_2}{f_1 + ba_o^2 (f_1^2 + f_2^2)} \tag{17}$$

Two methods were used to determine the displacement functions. Method A uses equations (15) and (17) while Method B uses equations (11) and (12).

(i) Method A

The solution of equations (15) and (17) for f_1 and f_2 has been determined by Chae (1964). An error, however, was found in his solution. The corrected solution appears in Appendix A, and follows the notation of Chae wherever possible. The solution gives two sets of values for f_1 and f_2. The theory, however, demands that f_1 be negative and f_2 positive. A computer program was written to determine the displacement

as well as other experimental results.. The program appears in Appendix D.

The experimental and theoretical values of the displacement function f_1 as a function of frequency factor are shown in Figure 20. The results of all five mass ratios are included in the diagram. The experimental results are close to the theoretical values for the frequency factor in the range of 0.3 to 0.4 which coincides with the range of the resonant frequencies. The displacement function f_1 is generally less than that predicted when the frequency is less than the resonant frequency and greater when higher than the resonant frequency. The difference is attributed to the fact that the predicted pressure distribution does not correspond to the actual pressure distribution.

The experimental and theoretical values of the displacement function f_2 versus frequency factor are shown in Figure 21. The experimental results follow the same general pattern as that predicted to the range of the resonant frequency. After the frequency factor has exceeded the range of the resonant frequency, the displacement function f_2 increases rapidly and then decreases rapidly to a value less than that predicted.

According to the Reissner-Sung theory, the displacement functions are independent of the mass ratio. Figure 20, however, shows that as the mass ratio increases the experimental value decreases for a given frequency factor. This trend is not as evident for the displacement function f_2 shown in Figure 21. Thus, it is evident that the displacement function is dependent upon the mass ratio. This dependence can be seen more clearly by examining the parameters a_o and b.

$$a_o = \omega r_o \sqrt{\frac{\rho}{G}} \tag{6}$$

$$b = \frac{m_o}{\rho r_o^3} \tag{7}$$

These parameters are not independent since G is a function of the confining pressure which is dependent upon the mass of the foundation m_o. This is the reason that the displacement functions are dependent upon the mass ratio.

A method of checking the reliability of f_1 and f_2 was used. The experimental values of f_1 and f_2 were substituted in equations (11) and (12) to determine the phase angle ϕ_{Q-R} and the soil reaction R_1. The results of this check are

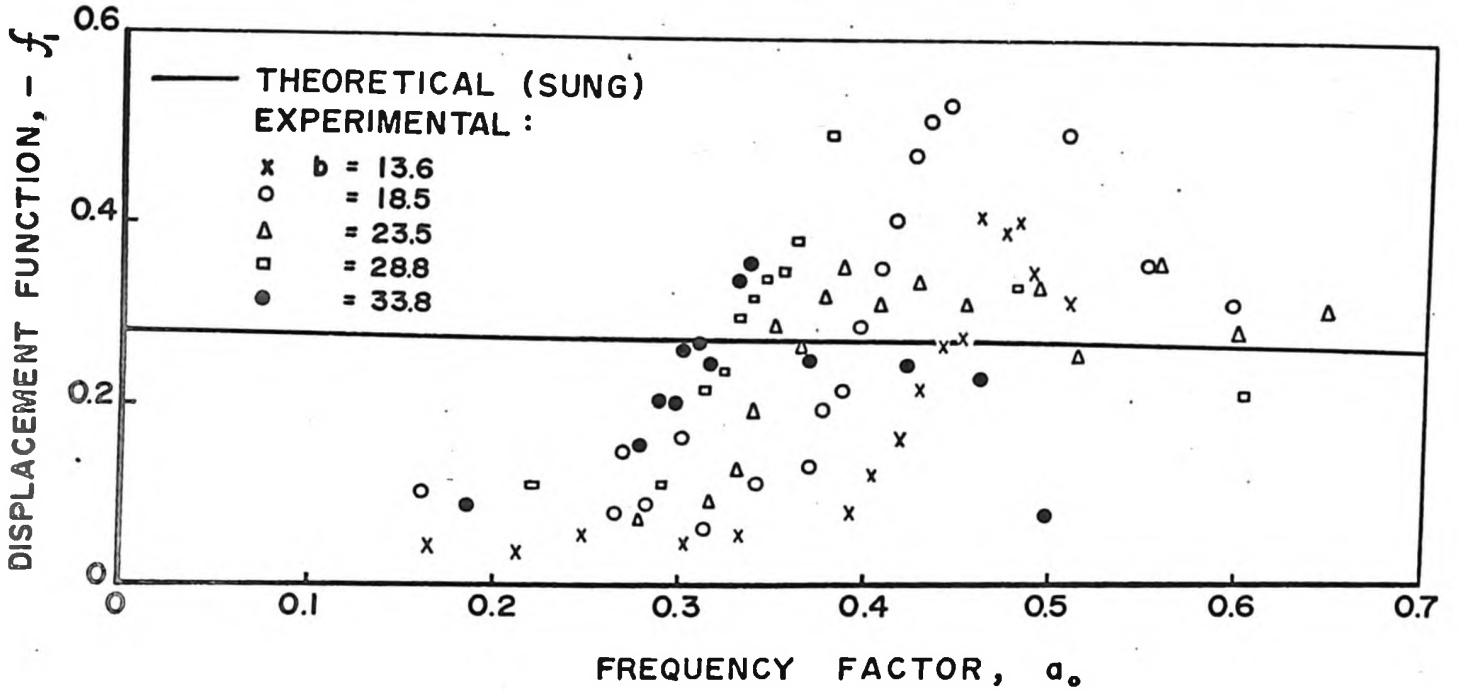

FIG. 20 EXPERIMENTAL AND THEORETICAL VALUES OF THE DISPLACEMENT FUNCTION f_1 VS. FREQUENCY FACTOR

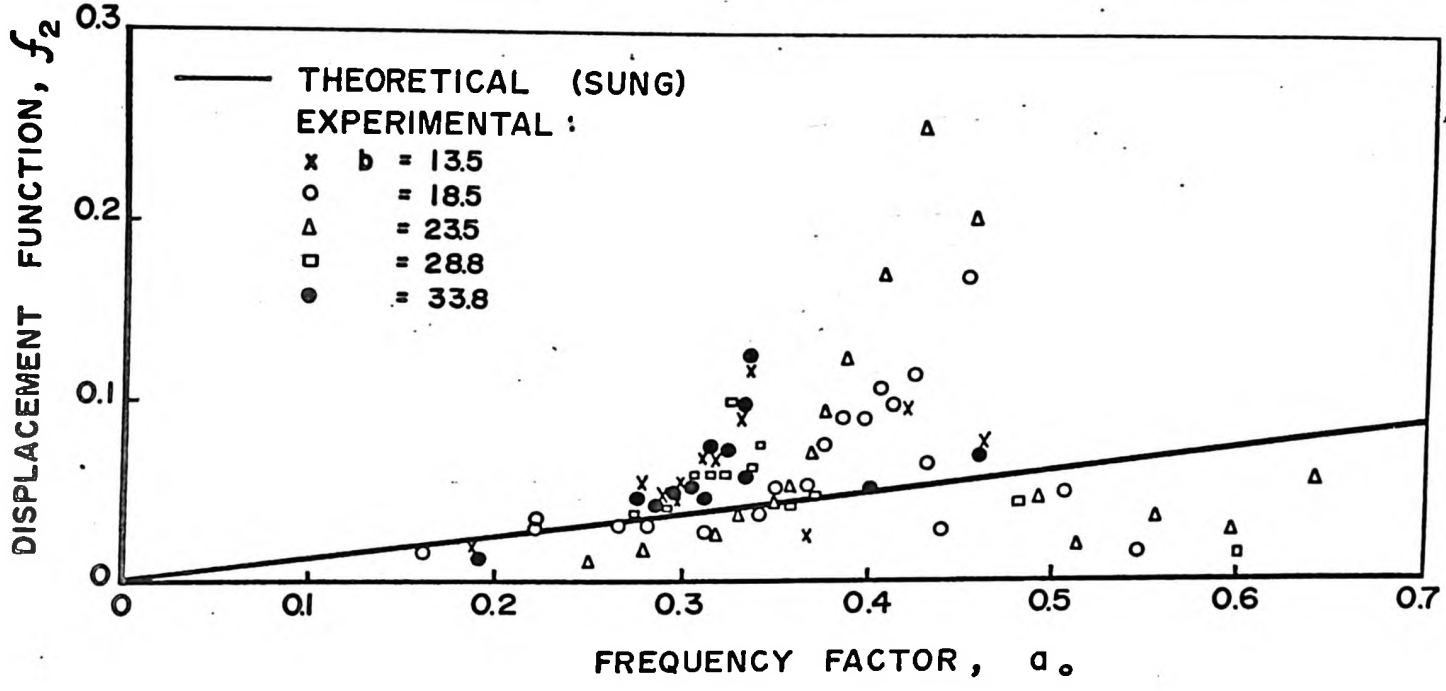

FIG. 21 EXPERIMENTAL AND THEORETICAL VALUES OF THE DISPLACEMENT FUNCTION f_2 VS. FREQUENCY FACTOR

shown as calculated points in Figure 15 and 19. Good agreement is obtained between the calculated and the experimental values. Although the displacement functions appear to have some scatter as shown in Figures 20 and 21, they are capable of predicting results in good agreement with that measured experimentally.

(ii) Method B

This method uses equations (11) and (12) to determine the displacement functions. The solution of these equations appears in Appendix B. As in Method A two sets of solutions for f_1 and f_2 exist but f_1 must be negative and f_2 positive. Results similar to those shown in Figures 20 and 21 were obtained. The values of f_1 and f_2 were substituted into equations (15) and (17) to determine respectively the amplitude of vibration and the phase angle, ϕ_{Q-x}. The results calculated for these equations are shown in Figures 13 and 14. The calculation of the phase angle ϕ_{Q-x} agrees quite well with that measured experimentally. The calculation of the amplitude of vibration is consistent with that measured experimentally except in the region of the resonant frequency.

Methods A and B have shown that by taking 2 of the 4 possible variables, and determining the displacement functions, the other two variables can be calculated. The calculated variables are in good agreement with the experimental variables. Thus, the experimentally determined displacement functions are capable of producing reliable predictions, even

though there seems to be some scatter in the displacement functions as shown in Figures 20 and 21. The results indicate that small fluctuations of the input variables produce magnified fluctuations in the determination of the displacement functions.

Resonant Frequency and Maximum Amplitude of Vibration

A comparison of the predicted and experimental resonant frequencies and maximum amplitudes of vibration is shown in Figure 22. As was predicted, the resonant frequency decreased as the mass ratio increased. The experimentally determined resonant frequencies are approximately 10 per cent lower than that predicted. Also as predicted, the maximum amplitude of vibration decreased as the mass ratio increased. The experimental values of the maximum amplitude of vibration are about 20 per cent less than that predicted.

A comparison of the experimental maximum amplitudes of vibration and resonant frequencies with that predicted by different types of pressure distribution are shown in Figure 23. The predicted results were determined using the Reissner-Sung theory with Sung's displacement functions for the three types of pressure distribution. The results show that the parabolic pressure distribution best predicts the response of the footing.

Settlement

Settlement of the footing occurred during the vibration tests. The settlement was noticed to be directly related to the amplitude of vibration with most of the settlement occurring at or near the resonant frequency. It was also observed that

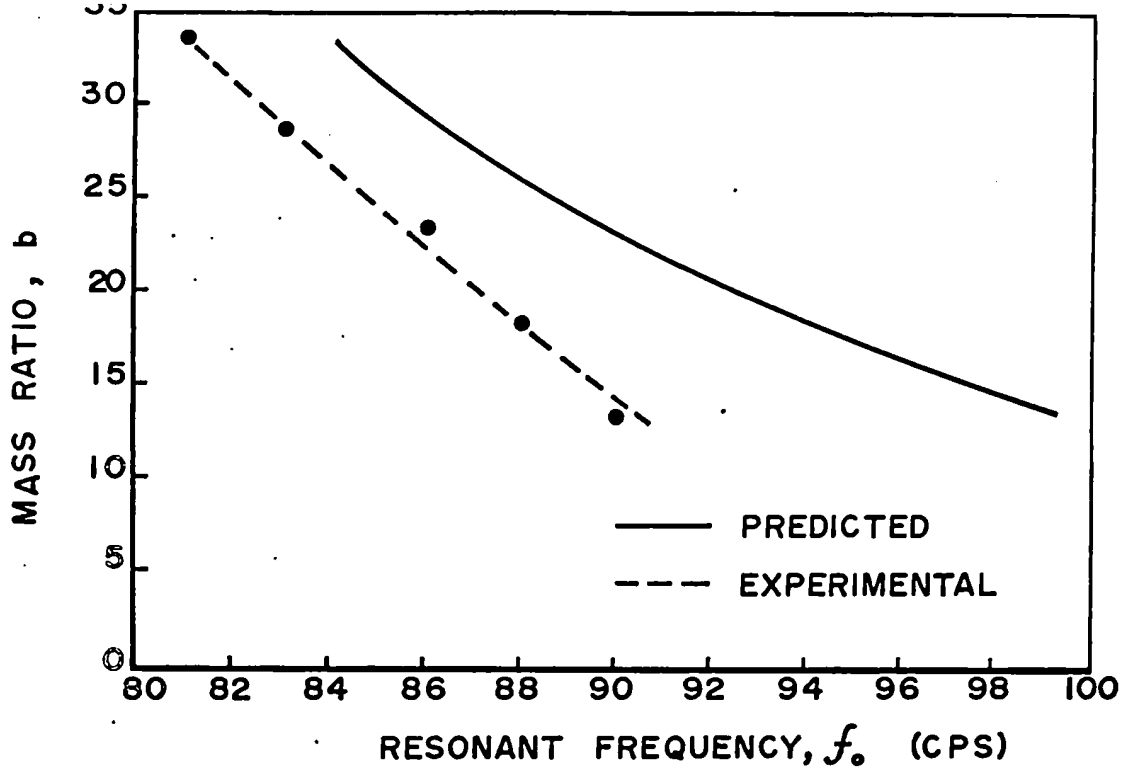

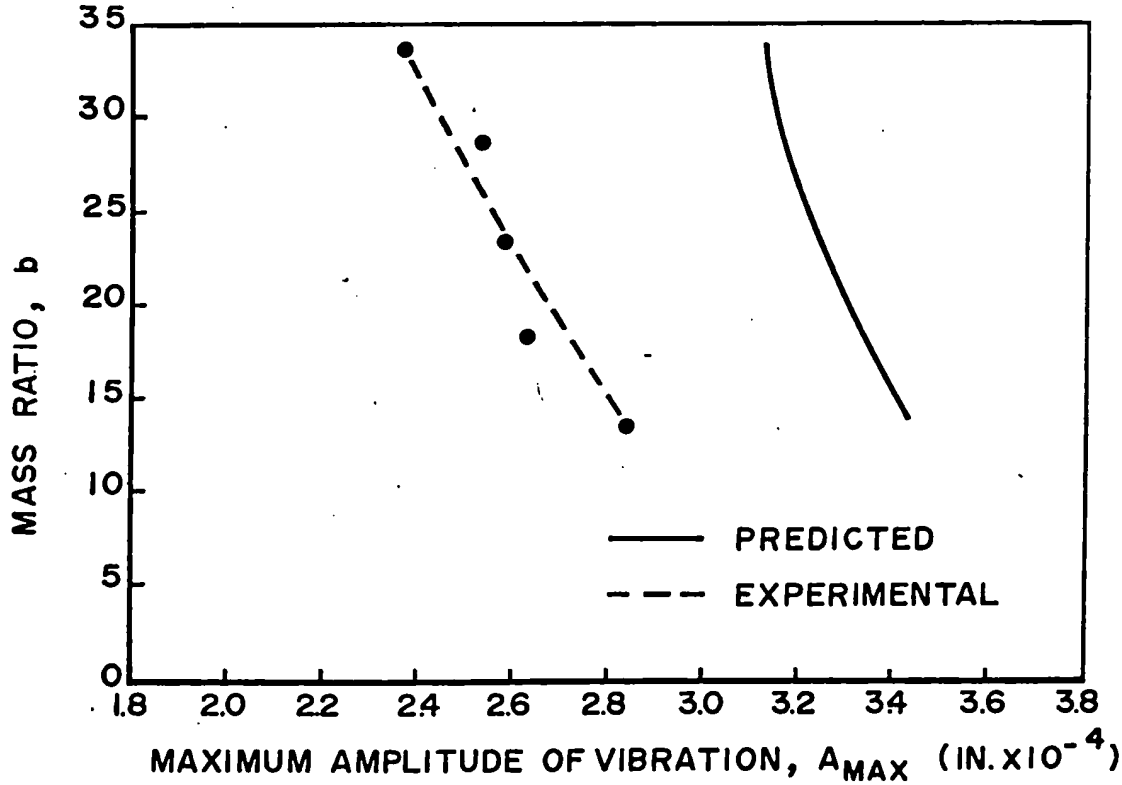

FIG. 22 EXPERIMENTAL AND PREDICTED RESONANT FREQUENCY AND MAXIMUM AMPLITUDE OF VIBRATION VS. MASS RATIO

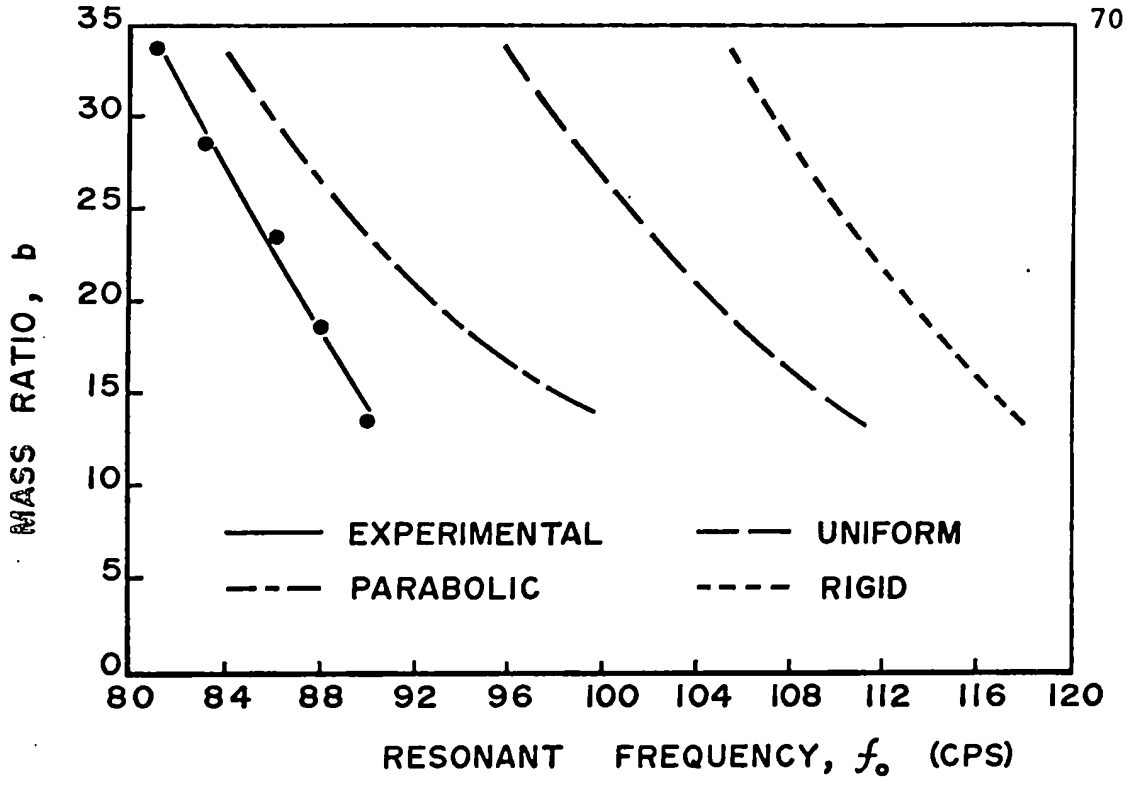

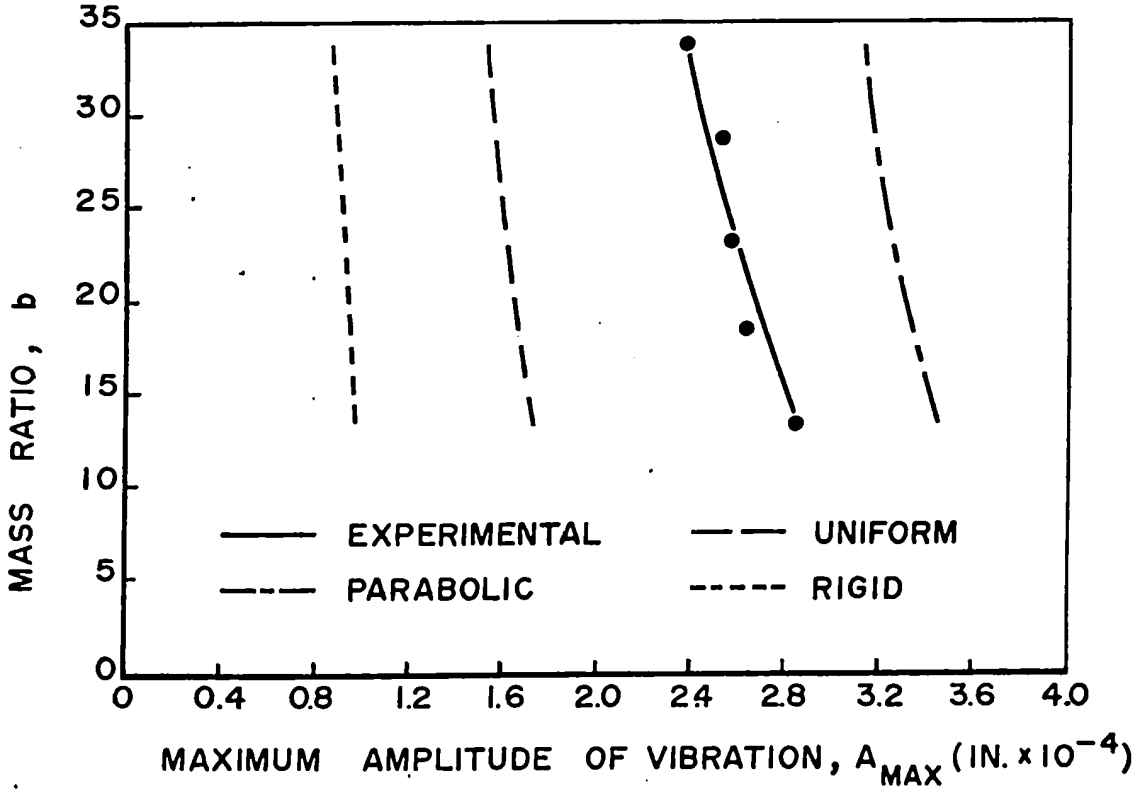

FIG. 23 EXPERIMENTAL AND PREDICTED RESONANT FREQUENCY AND MAXIMUM AMPLITUDE OF VIBRATION VS. MASS RATIO FOR DIFFERENT TYPES OF PRESSURE DISTRIBUTION

at a given frequency the settlement occurred rapidly and then reached a near steady-state value. Settlement was measured with a deflectometer during two tests each having a mass ratio of 13.5. The results showed total settlements of 1/3 and 1/2 of an inch.

CHAPTER 7

CONCLUSIONS AND RECOMMENDATIONS

Conclusions

The following conclusions are derived from the foundation-soil system used in this research program. The foundation consisted of a rigid circular footing resting on the surface of a cohesionless soil. The footing was subjected to a constant vertical force.

(A) The magnitude of the contact pressure on the foundation-soil interface is a function of frequency. The maximum value occurs at the resonant frequency.

(B) The contact pressure distribution is a function of frequency. The pressure at the centre of the foundation is a maximum and decreases to a minimum at the edge. An intermediate minimum pressure occurs at resonant frequencies up to and including the resonant frequency.

(C) The contact pressure acts in phase across the foundation-soil interface.

(D) Experimental determination of the displacement functions is difficult due to their sensitivity to fluctuation of the experimental data.

(E) Contrary to the Reissner-Sung theory, the displacement functions are dependent upon the mass ratio.

(F) The Reissner-Sung theory assuming parabolic pressure distribution gives conservative predictions of the resonant frequency, amplitude of vibration and soil reaction.

The resonant frequency and maximum amplitude of vibration can be expected to be respectively about 10 and 20 per cent lower than that predicted.

(G) Differences between the experimental and predicted results are attributed to the differences in the dynamic pressure distribution. The dynamic pressure distribution is not exactly parabolic as predicted.

Recommendations

It is recommended that research be conducted concerning the settlement of foundations when subjected to vibratory loads. Effects of amplitude of vibration and time should be included in the investigation.

Further investigations are needed to predict the dynamic response of foundation-soil systems under conditions different from those considered herein. The effects of the geometry of foundation, embedment of foundation, different types of soil, and different modes of vibration should be included in these investigations.

REFERENCES

Arnold, R. N., Bycroft, G. N. and Warburton, G. B. (1955). "Forced Vibrations of a Body on an Infinite Elastic Solid"; J. Appl. Mech., Trans, ASME, vol. 77, p.391-400.

Chae, Y. S. (1964). "Dynamic Pressure Distribution at the the Base of a Rigid Footing Subjected to Vibratory Loads"; Ph.D. Thesis, University of Michigan.

Crockett, S. H. A. and Hammond, R. E. R. (1948). "The Natural Oscillation of Ground and Industrial Foundations"; Proc. 2nd Int. Conference Soil Mech. and Found. Eng., vol. 3, p. 88-93.

Drnevich, V. P., Hall, J. R.,Jr., and Richart, F. E., Jr. (1966). "Transient Loading Tests on a Rigid Circular Footing"; U.S. Army Engineer Waterways Experiment Station, Vicksbury, Miss.

Faber, O. (1933). "Pressure Distribution Under Bases and Stability of Foundations"; Structural Engineer, vol. 11 (New Series), no. 3, p. 82-98.

Fry, Z. B. (1963). "Development and Evaluation of Soil Bearing Capacity, Foundations of Structures - Field Vibratoty Test Data"; Technical Report No. 3-632, U.S. Army Engineer Waterways Experiment Station, Vicksburg, Miss.

Hall, J. R., Jr. and Richart, F. E., Jr. (1963). "Effect of Vibration Amplitude on Wave Velocities in Granular Materials"; Proc. 2nd Panamerican Conf. on Soil Mech. and Found. Eng., vol. 1, p. 145-162.

Hardin, B. O. (1965). "Dynamic vs. Static Shear Modulus for Dry Sand"; Materials Research and Standards, ASTM, May 1965.

Hardin, B. O. and Richart, F.E., Jr. (1963). "Elastic Wave Velocities in Granular Soils"; ASCE Soil Mech. and Found. Div., p. 33-65, Feb. 1963.

Hertwig, A., Früh, G. and Lorenz, H. (1933). "Die Ermittlung der für das Bauwesen wichtigsten Eigenschaften des Bodens durch erzwungene Schwingungen"; DEGEBO, no. 1, J. Springer, Berlin.

Ho, M. M.K. and Burwash, W. J. (1968). "Vertical Vibration of a Rigid Foundation Resting on Sand"; (Accepted for presentation and publication), Symposium on Earthquake and Vibration Effects on Soils and Foundations, ASTM, June 1968.

Ho, M. M.K., Lopes, R. and Burwash, W. J. (1968). "Static Contact Pressure Distribution"; (in preparation for publication).

Leonards, G. A. (1962). "Foundation Engineering"; McGraw-Hill, New York.

Lysmer, J. and Richart, F. E., Jr. (1966). "Dynamic Response of Footings to Vertical Loading"; ASCE Soil Mechanics and Found. Div., p. 65-91, Jan. 1966.

Pauw, A. (1953). "A Dynamic Analogy for Foundation-Soil Systems"; Symposium on Dynamic Testing of Soils, ASTM STP, no. 156, p. 90-112.

Phalen, T. E., Jr. (1963), discussion of "Elastic Wave Velocities in Granular Soils" by Hardin, G. O. and Richart, F. E., Jr., ASCE Soil Mechanics and Found. Div., p. 33-65, Feb. 1963.

Reissner, E. (1936). "Stationäre, axialsymmetrische, durch eine schüttelnde Masse erregte Schwingungen eines homogenen elastischen Halbraumes"; Ingenieur-Archiv, vol. 7, no. 6, p. 381-396, Berlin, West Germany.

Richart, F. E., Jr. (1960). "Foundation Vibrations"; ASCE Soil Mechanics and Found. Div., p. 1-34, Aug. 1960.

Richart, F. E., Jr. and Whitman, R. V. (1967). "Comparison of Footing Vibration Tests with Theory"; ASCE Soil Mechanics and Found. Div., p. 143-168, Nov. 1967.

Sung, T. Y. (1953). "Dynamic Testing of Soils: Vibrations in Semi-Infinite Solids due to Periodic Surface Loading"; Symposium on Dynamic Testing of Soils, ASTM STP no. 156, p. 35-63.

Warburton, G. B. (1957). "Forced Vibrations of a Body upon an Elastic Stratum"; Journal of Applied Mechanics, vol. 24, p. 55-58.

Whitman, R. V. (1966). "Analysis of Foundation Vibrations" Vibration in Civil Engineering, Butterworths, London.

APPENDIX A

FIRST DETERMINATION OF THE DISPLACEMENT FUNCTIONS

Equations (15) and (17) are used to solve for f_1 and f_2.

$$X = \frac{Q_1}{Gr_o}\sqrt{\frac{f_1^2 + f_2^2}{(1 + ba_o^2 f_1)^2 + (ba_o^2 f_2)^2}} \tag{A-1}$$

$$\tan \phi_Q - x = \frac{- f_2}{f_1 + ba_o^2(f_1^2 + f_2^2)} \tag{A-2}$$

By rearranging and squaring (A-1)

$$\left(\frac{XGr_o}{Q_1}\right)^2 = \frac{f_1^2 + f_2^2}{(1 + ba_o^2 f_1)^2 + (ba_o^2 f_2)^2} \tag{A-3}$$

Let

$$D = ba_o^2 \tag{A-4}$$

$$M = \left(\frac{XGr_o}{Q_1}\right)^2 \tag{A-5}$$

$$N = \tan \phi_Q - x \tag{A-6}$$

and substituting in (A-2) and (A-3)

$$\frac{- f_2}{f_1 + D(f_1^2 + f_2^2)} = N \tag{A-7}$$

$$\frac{f_1^2 + f_2^2}{(1 + Df_1)^2 + (Df_2)^2} = M \tag{A-8}$$

From (A-8)

$$f_1^2 + f_2^2 = M(1 + Df_1)^2 + M(Df_2)^2$$

$$= M + 2MDf_1 + MD^2f_1^2 + MD^2f_2^2$$

$$= M + 2MDf_1 + MD^2(f_1^2 + f_2^2)$$

$$MD^2(f_1^2 + f_2^2) - (f_1^2 + f_2^2) + M + 2MDf_1 = 0$$

$$(f_1^2 + f_2^2)\ (MD^2 - 1) + 2MDf_1 + M = 0 \qquad \text{(A-9)}$$

From (A-7)

$$- f_2 = Nf_1 + ND(f_1^2 + f_2^2)$$

$$(f_1^2 + f_2^2)ND + Nf_1 + f_2 = 0 \qquad \text{(A-10)}$$

Let

$$C = MD^2 - 1 \qquad \text{(A-11)}$$

$$E = 2\ DM \qquad \text{(A-12)}$$

and substituting in (A-9) and (A-10)

$$C(f_1^2 + f_2^2) + Ef_1 + M = 0 \qquad \text{(A-13)}$$

$$ND(f_1^2 + f_2^2) + Nf_1 + f_2 = 0 \qquad \text{(A-14)}$$

(A-13) x $(\frac{ND}{C})$

$$ND(f_1^2 + f_2^2) + \frac{END}{C} f_1 + \frac{MND}{C} = 0 \qquad \text{(A-15)}$$

(A-15) - (A-14)

$$\left(\frac{END}{C} - N\right) f_1 - f_2 + \frac{MND}{C} = 0$$

$$f_2 = \left(\frac{END}{C} - N\right) f_1 + \frac{MND}{C} \qquad \text{(A-16)}$$

Let

$$H = \frac{ND}{C} \qquad \text{(A-17)}$$

$$T = [b^2 a_o^4 \left(\frac{XGr_o}{Q_1}\right)^2 - 1] + \tan^2\phi_Q - x\left[b^2 a_o^4 \left(\frac{XGr_o}{Q_1}\right)^2 + \frac{4}{b^2 a_o^4 \left(\frac{XGr_o}{Q_1}\right)^2} + 3\right]$$

$$Q = \frac{b^2 a_o^4 \left(\frac{XGr_o}{Q_1}\right)^4 \tan^2\phi_Q - x}{b^2 a_o^4 \left(\frac{XGr_o}{Q_1}\right)^2 - 1} + \left(\frac{XGr_o}{Q_1}\right)^2$$

$$K = \frac{2b^2 a_o^4 \left(\frac{XGr_o}{Q_1}\right)^2 \tan\phi_Q - x}{b^2 a_o^4 \left(\frac{XGr_o}{Q_1}\right)^2 - 1} - \tan\phi_Q - x$$

$$S = \frac{b\, a_o^2 \left(\frac{XGr_o}{Q_1}\right)^2 \tan\phi_Q - x}{b^2 a_o^4 \left(\frac{XGr_o}{Q_1}\right)^2 - 1}$$

APPENDIX B

SECOND DETERMINATION OF THE DISPLACEMENT FUNCTIONS

Equations (11) and (12) are used to solve for f_1 and f_2.

$$\phi_{Q-R} = \tan^{-1} \frac{ba_o^2 f_2}{1 + ba_o^2 f_1} \tag{B-1}$$

$$R_1 = \frac{Q_1}{\sqrt{(1 + ba_o^2 f_1)^2 + (ba_o^2 f_2)^2}} \tag{B-2}$$

Let

$$A = 1 + ba_o^2 f_1 \tag{B-3}$$

$$B = ba_o^2 f_2 \tag{B-4}$$

and substituting in (B-1) and (B-2)

$$\phi_{Q-R} = \tan^{-1} \frac{B}{A} \tag{B-5}$$

$$R_1 = \frac{Q_1}{\sqrt{A^2 + B^2}} \tag{B-6}$$

Rearranging (B-6)

$$A^2 + B^2 = \left(\frac{Q_1}{R_1}\right)^2 \tag{B-7}$$

Let

$$C^2 = \left(\frac{Q_1}{R_1}\right)^2 \tag{B-8}$$

and substituting in (B-7) and rearranging

$$B^2 = C^2 - A^2 \tag{B-9}$$

from (B-5)

$$A = B \cot \phi_{Q-R} \tag{B-10}$$

substituting (B-10) in (B-9)

$$B^2 = C^2 - B^2 \cot^2\phi_{Q-R}$$

$$B = \pm\sqrt{\frac{C^2}{1 + \cot^2 \phi_{Q-R}}} \qquad \text{(B-11)}$$

substituting (B-4) in (B-11)

$$ba_o^2 f_2 = \pm\sqrt{\frac{C^2}{1 + \cot^2 \phi_{Q-R}}}$$

$$f_2 = \pm \frac{C}{ba_o^2}\sqrt{\frac{1}{1 + \cot^2 \phi_{Q-R}}}$$

$$= \pm \frac{Q_1}{ba_o^2 R_1}\sqrt{\frac{1}{1 + \cot^2 \phi_{Q-R}}} \qquad \text{(B-12)}$$

substituting (B-12) in (B-11)

$$A = \pm \cot \phi_{Q-R}\sqrt{\frac{C^2}{1 + \cot^2\phi_{Q-R}}} \qquad \text{(B-13)}$$

substituting (B-3) in (B-11)

$$1 + ba_o^2 f_1 = \pm \cot \phi_{Q-R}\sqrt{\frac{C^2}{1 + \cot^2 \phi_{Q-R}}}$$

$$f_1 = \frac{Q_1 \cot \phi_{Q-R}}{ba_o^2 R_1}\sqrt{\frac{1}{1 + \cot^2 \phi_{Q-R}}} - \frac{1}{ba_o^2} \qquad \text{(B-14)}$$

APPENDIX C

COMPUTER PROGRAM FOR PREDICTED RESPONSE

```
      PREDICTIONS USING REISSNER-SUNG THEORY
   SOLUTION ASSUMES PARABOLIC PRESSURE DISTRIBUTION
         POISSON RATIO = 1/3

      DO 100 II=1,5
      READ(5,10) W,Q,AO1
      W IS WEIGHT OF FOUNDATION IN LBS
      Q IS AMPLITUDE OF INPUT FORCE
      AO1 IS FREQUENCY FACTOR
   10 FORMAT(3F10.2)
      GAMMA IS UNIT WEIGHT OF SOIL
      GAMMA=110.0
      RO IS RADIUS OF FOOTING
      RO=2.9375
      ROF=2.9375/12.0
      B IS MASS RATIO
      B=W/(GAMMA*ROF**3)
      E IS VOID RATIO OF SOIL
      E=0.51
   48 WRITE(6,49)
   49 FORMAT(1H1)
      WRITE(6,50) W
   50 FORMAT(1X,59HTHEORETICAL RESPONSE FOR CIRCULAR FOOTING OF WEIGHT (
     1LBS) =,F7.2)
      WRITE(6,51) Q,B
   51 FORMAT(1X,19HINPUT FORCE (LBS) =,F6.2,5X,12HMASS RATIO =,F6.2)
      WRITE(6,52)
   52 FORMAT(1X,63HASSUMING PARABOLIC PRESSURE DISTRIBUTION AND POISSON
     1RATIO=0.33)
      WRITE(6,55)
   55 FORMAT(1X, 59HSOIL IS OTTAWA STANDARD SAND WITH UNIT WEIGHT OF 110
     1 LB/FT3)
  110 WRITE(6,54)
  54  FORMAT(1X,81HASSUMING CONFINIG PRESSURE = 1/2 AVERAGE NORMAL STRES
     1S TO CALCULATE SHEAR MODULUS///)
  100 WRITE(6,70)
  700 FORMAT(10X,9HFREQUENCY,5X,16HFREQUENCY FACTOR,5X,22HDISPLACEMENT F
     1UNCTIONS,5X,12HPHASE ANGLES,5X,13HSOIL REACTION,5X,22HAMPLITUDE OF
     2 VIBRATION)
      WRITE(6,71)
  71  FORMAT(13X,3HCPS,32X,2HF1,10X,2HF2,7X, 5HPHIRX, 2X, 5HPHIQR, 2X,
     15HPHIQX, 5X, 3HLBS, 18X, 6HINCHES/)
      CONFINING PRESSURE = 0.5 * AVERAGE NORMAL PRESSURE
      SIGMAO=W/(3.14159*ROF**2)
  8   CAPPA=0.5
      CONF2=CAPPA*SIGMAO
      G1=(22.52-10.60*E)**2
      E=0.51
      G2=1.0+E
```

```
      GPS1=(G1/G2)*CONF2**0.6
      GPSF IS SHEAR MODULUS IN LB/FT2
      GPSF=GPS1*144.0
      FREQ IS FREQUENCY
   16 FREQ=-1.0
   17 DELTAF=1.0
      FREQ=FREQ+DELTAF
      RHO IS MASS DENSITY OF SOIL
      RHO=GAMMA/32.2
      AO IS FREQUENCY FACTOR
      AO=2.0*3.14159*FREQ*ROF*SQRT(RHO/GPSF)
      DF1 AND DF2 ARE THE DISPLACEMENT FUNCTIONS
      DF1 =-(0.282942-0.041262*AO*AO+0.001973*AO**4)
      DF2 =0.130630*AO-0.010024*AO**3+0.000328*AO**5
      PH1RX=ATAN(-DF2/DF1)
      CHANGE FROM RADIANS TO DEGREES
      PH1RXD=57.29577*PH1RX
      PH1QR1=B*AO*AO*DF2
      PH1QR2=1.0+B*AO*AO*DF1
      PH1QR=ATAN(PH1QR1/PH1QR2)
      PH1QRD=57.29577*PH1QR
      IF(PH1QRD.LT.0.0) PH1QRD=180.0+PH1QRD
      PH1QX1=-DF2
      PH1QX2=DF1+B*AO*AO*(DF1*DF1+DF2*DF2)
      PH1QX=ATAN(PH1QX1/PH1QX2)
      PH1QXD=57.29577*PH1QX
      IF(PH1QXD.LT.0.0) PH1QXD=180.0+ PH1QXD
      CALCULATION OF SOIL REACTION  R
      R=Q/SQRT(PH1QR2**2+PH1QR1**2)
      CALCULATION OF AMPLITUDE OF VIBRATION
      DISPL1=DF1*DF1+DF2*DF2
      DISPL2=PH1QR2**2+PH1QR1**2
      DISPL=Q/(GPSF*ROF)*SQRT(DISPL1/DISPL2)
      DISPF=DISPL
      DISPIN=DISPL*12.0
      WRITE(6,60) FREQ,AO,DF1,DF2,PH1RXD,PH1QRD,PH1QXD,R,DISPIN
   60 FORMAT(11X, F6.1, 12X, F6.3, 11X, F6.3, 6X, F6.3, 4X, F6.1, 1X,
     1F6.1, 1X, F6.1, 3X, F7.3, 15X, E10.3)
      IF(FREQ.LT.200.0) GO TO 17
      CALCULATION OF RESONANT FREQUENCY AND MAXIMUM AMPLITUDF
      I=1
      DELTA=0.001
   80 DF11=-(0.282942-0.041262*AO1*AO1+0.001973*AO1**4)
      DF21=0.130630*AO1-0.010024*AO1**3+0.000328*AO1**5
      T=DF11*DF11 + DF21*DF21
      D1=(1.0+B*AO1*AO1*DF11)**2
      D2=(B*AO1*AO1*DF21)**2
      A21=SQRT(T/(D1+D2))
      AO1=AO1+DELTA
      I=I+1
      IF(I.GT.1000) GO TO 30
      DF11=-(0.282942-0.041262*AO1*AO1+0.001973*AO1**4)
      DF21=0.130630*AO1-0.010024*AO1**3+0.000328*AO1**5
      T=DF11*DF11 +.DF21*DF21
```

```
      D1=(1.0+B*A01*A01*DF11)**2
      D2=(B*A01*A01*DF21)**2
      A2=SQRT(T/(D1+D2))
      IF(ABS(A2-A21).LT.0.00000001) GO TO 30
      IF(A2.LE.A21) GO TO 90
      GO TO 80
   0  A01=A01-DELTA
      DELTA=0.1*DELTA
      GO TO 80
   0  ROOT=SQRT(GPSF/RHO)
      RFREQ=A01/(2.0*3.14159*ROF)*ROOT
      X1=DF11*DF11+DF21*DF21
      X2=(1.0+B*A01*A01*DF11)**2+(B*A01*A01*DF21)**2
      X=Q/(GPSF*ROF)*SQRT(X1/X2)
      XIN=X*12.0
      WRITE(6,31) RFREQ, XIN
    1 FORMAT(40X,26HRESONANT FREQUENCY (CPS) =,F6.1/40X,41HMAXIMUM AMPLI
     1TUDE OF VIBRATION (INCHES) =,E10.3)
    9 WRITE(6,98)
    8 FORMAT(1H1)
  100 CONTINUE
      STOP
      END
```

APPENDIX D

COMPUTER PROGRAM FOR EXPERIMENTAL RESPONSE

```
                FINAL DATA SERIES I
   DOUBLE PRECISION G, A3, A1, A1A1, A2, A2A2, A3A3, Y1, Y2, Y3, Y,
  1TT1, TT2, TT3, TT4, T, Q1, Q2, QQ, C1, C2, C, S1, S2, S, QUAD,
  2F11, F12, F21, F22, PHIQXR
   DOUBLE PRECISION COT, DF1, DF2, PHIQRR
   K IS NUMBER OF SETS OF DATA /2
   DO 100 K=1,11
   WRITE(6,20)
20 FORMAT(1H1)
   DO 100 N=1,2
    W=WEIGHT OF FOOTING
   W=21.7
   READ (5,10) FREQ, DTR1, DTR2, DTRPRE, PHIQXD, PHIQRD, T11, T12,
  1PREAP1, T21, T22, PREAP2, T31, T32, PREAP3, T41, T42, PREAP4,
  2T51, T52, PREAP5, T61, T62, PREAP6
10 FORMAT( F10.1, 3F5.2/ 2F10.1/ 9F5.2/9F5.2)
   RO=2.9375
   RO=RADIUS OF FOOTING IN INCHES
   RO3=(2.9375/12.0)**3
   GAMMA=110.0
   B=MASS RATIO
   B=W/(GAMMA*RO3)
   Q IS AMPLITUDE OF DYNAMIC FORCE
   QR=0.25
   QRPRE=0.2
   QRAMP=1.0
   Q=QR*36.8*(QRPRE*QRAMP)
   QR IS IN CENTIMETERS
   CALCULATION OF DYNAMIC SHEAR MODULUS
   E=VOID RATIO
   E=0.51
   SIGMAO=AVERAGE NORMAL STRESS IN LB/FT2
   SIGMAO=W/(3.14159*(RO/12.0)**2)
   CAPPA=CONFINING PRESSURE CORRECTION FACTOR
   CAPPA=0.5
   CONF=CONFINING PRESSURE
   CONF=CAPPA*SIGMAO
   G1=(22.52-10.60*E)**2
   G2=1.0+E
   G=(G1/G2)*CONF**0.6
   G IS IN LB/IN2
   CALCULATION OF FREQUENCY FACTOR AO
   GPSF=G*144.0
   RHO=GAMMA/32.2
   ROF=RO/12.0
   AO=2.0*3.14159*FREQ*ROF*SQRT(RHO/GPSF)
   CALCULATION OF DISPLACEMENT AMPLITUDE AND ACCELERATION
   DTR=(DTR1 + DTR2)/2.0
```

```
      DTRAMP=1.0
      DISPL=DTR*1.05E-04*(DTRPRE*DTRAMP)
      DISPLF=DISPL/12.0
      ACCEL=DISPLF*(2.0*3.14159*FREQ)**2
      ACCELERATION IS IN FT/SEC2

      CHANGE PHASE ANGLES FROM DEGREES TO RADIANS
      PHIQXR=PHIQXD/(180.0/3.14159265358979320D0)
      PHIQRR=PHIQRD/(180.0/3.14159265358979320D0)

      DYNAMIC PRESSURE DISTRIBUTION
      T1 TO T6 ARE THE DYNAMIC PRESSURE AMPLITUDES
      AMP1=0.1
      AMP2=0.1
      AMP3=0.1
      AMP4=0.1
      AMP5=0.1
      AMP6=0.1
      T1=0.5*1.23*(T12+T11)*(PREAP1*AMP1)
      T2=0.5*1.03 *(T22+T21)*(PREAP2*AMP2)
      T3=0.5*6.59*(T32+T31)*(PREAP3*AMP3)
      T4=0.5*6.02*(T42+T41)*(PREAP4*AMP4)
      T5=0.5*3.70*(T52+T51)*(PREAP5*AMP5)
      T6=0.5*4.44*(T62+T61)*(PREAP6*AMP6)

      CALCULATION OF TOTAL DYNAMIC SOIL REACTION
      ORD1=(T3+T4)/2.0
      AREA1=3.14159*0.75**2
      VOL1=ORD1*AREA1
      ORD2=(T3+T5)/2.0
      AREA2=3.14159*(1.0**2-0.75**2)
      VOL2=ORD2*AREA2
      ORD3=(T2+T5)/2.0
      AREA3=3.14159*(1.5**2-1.0**2)
      VOL3=ORD3*AREA3
      ORD4=(T6+T2)/2.0
      AREA4=3.14159*(2.0**2-1.5**2)
      VOL4=ORD4*AREA4
      ORD5=(T1+T6)/2.0
      AREA5=3.14159*(2.5625**2-2.0**2)
      VOL5=ORD5*AREA5
      ORD6=T1/2.0
      AREA6=3.14159*(2.9375**2-2.5625**2)
      VOL6=ORD6*AREA6
      R=VOL1+VOL2+VOL3+VOL4+VOL5+VOL6
      R=SOIL REACTION
      EFMASS= R - Q*COS(PHIQXD)
      RMASS=(W/32.2)*ACCEL
      DIFF=EFMASS-RMASS
      DIFFPC=(DIFF/EFMASS)*100.0

      WRITE(6,50) W, B, Q
   50 FORMAT(//13X, 25HWEIGHT OF FOOTING (LBS) =, F6.2, 9X,
     1 11HMASS RATIO=,
```

```
  2F6.2, 10X, 32HAMPLITUDE OF INPUT FORCE (LBS) =, F6.2)
   WRITE(6,51) GAMMA, G
51 FORMAT(24X, 26HDENSITY OF SOIL (LB/FT3) =, F6.1, 20X, 24HSHEAR MOD
  2ULUS (LB/IN2) =,F8.1//)
   WRITE(6,52)
52 FORMAT(6X, 9HFREQUENCY, 5X, 12HACCELERATION, 4X, 12HAMPLITUDE OF,
  15X, 8HPHI(Q-X), 5X, 8HPHI(Q-R), 5X, 9HFREQUENCY, 10X, 22HDISPLACEM
  2ENT FUNCTIONS)
   WRITE(6,53)
53 FORMAT(9X, 3HCPS, 11X, 7HFT/SEC2, 4X, 16HDISPLACEMENT IN., 3X,
  17HDEGREES, 6X, 7HDEGREES, 7X, 6HFACTOR, 10X, 7HF1(-VE), 9X,
  27HF2(+VE)/)

   DETERMINATION OF DISPLACEMENT FUNCTIONS
   A1=(DISPL*G*RO/Q)**2
   A1A1=A1*A1
   A2=B*AO*AO
   A2A2=A2*A2
   A3=TAN(PHIQXR)
   A3A3=A3*A3

   Y1=2.0*A2*A1
   Y2=A3A3*(A2A2*A1+1.0)
   Y3=A2A2*A1-1.0
   Y=Y1*(1.0+Y2/Y3)
   TT1=A2A2*A1-1.0
   TT2=A2A2*A1*A3+A3
   TT3=TT2*TT2
   TT4=A2A2*A1-1.0
   T=TT1+TT3/TT4
   IF(T.EQ.0.0) GO TO 72
   Q1=A2*A2*A1*A1*A3*A3
   Q2=A2*A2*A1-1.0
   QQ=Q1/Q2+A1
   C1=2.0*A2*A2*A3*A1
   C2=A2*A2*A1-1.0
   C=C1/C2-A3
   S1=A2*A1*A3
   S2=A2*A2*A1-1.0
   S=S1/S2
   QUAD=Y*Y-4.0*T*QQ
   IF(QUAD.LT.0.0) GO TO 80
   F11=(-Y+DSQRT(QUAD))/(2.0*T)
   F12=(-Y-DSQRT(QUAD))/(2.0*T)
   F21=C*F11+S
   F22=C*F12+S
   GO TO 73
72 F11=-QQ/Y
   F12=0.0
   F21=C*F11 + S
   F22=0.0
73 WRITE(6,54)FREQ, ACCEL, DISPL, PHIQXD, PHIQRD, AO, F11, F12,
  1F21, F22
54 FORMAT(7X, F6.1, 7X, F9.6, 6X, E10.3, 8X, F6.1, 7X, F6.1, 8X, F6.3
  1, 7X, F7.3,
```

```
     22X, F7.3, 2X, F7.3, 2X, F7.3//)
      GO TO 90
   80 QUAD=0.0
      F11=(-Y)/(2.0*T)
      F12=F11
      F21=C*F11+S
      F22=F21
      WRITE(6,55) FREQ, ACCEL, DISPL, PHIQXD, PHIQRD, AO, F11, F12,
     1F21, F22
   55 FORMAT(7X, F6.1, 7X, F9.6, 6X, E10.3, 8X, F6.1, 7X, F6.1, 8X, F6.3
     1, 7X, F6.3,
     21HI, 1X, F6.3, 1HI, 1X, F6.3, 1HI, 1X, F6.3, 1HI//)
   90 WRITE(6,56)
   56 FORMAT(70X, 30HTRANSDUCER NUMBER AND LOCATION)
      WRITE(6,57)
   57 FORMAT(49X, 6HT4(0R), 5X, 9HT3(0.75R), 5X, 8HT5(1.0R), 5X, 9HT2(1.
     150R), 5X, 8HT6(2.0R), 5X, 11HT1(2.5625R)/)
      WRITE(6,58) T4, T3, T5, T2, T6, T1
   58 FORMAT(5X, 35HDYNAMIC PRESSURE AMPLITUDE (LB/IN2), 9X, F6.2,
     16X, F6.2, 8X, F6.2, 7X, F6.2,   8X, F6.2, 8X, F6.2//)
      WRITE(6,61)
   61 FORMAT(13X, 25HDYNAMIC SOIL REACTION (R), 10X, 15HINPUT FORCE (Q),
     110X, 19HMASS X ACCELERATION, 8X, 3HQ-R, 10X, 10HDIFFERENCE)
      WRITE(6,62)
   62 FORMAT(23X, 3HLBS, 28X, 3HLBS, 24X, 3HLBS, 16X, 3HLBS,11X, 8HPER C
     1ENT/)
      WRITE(6,63) R, Q, RMASS, EFMASS, DIFFPC
   63 FORMAT(20X, F7.2, 25X, F6.2, 20X, F7.2, 12X, F7.2, 10X, F7.2/)

      METHOD A
      CALCULATION OF PHIQR AND R FROM F1 AND F2
      FIQR11=B*AO*AO*F21
      FIQR21=1.0+B*AO*AO*F11
      FIQR1=ATAN(FIQR11/FIQR21)
      FIQR1D=57.29577*FIQR1
      IF(FIQR1D.LT.0.0) FIQR1D= FIQR1D+180.0
      R1=Q/SQRT(FIQR21**2+FIQR11**2)
      WRITE(6,130) FIQR1D, R1
  130 FORMAT(1X, 26H USING F11 AND F21, PHIQR=, F7.1, 5X, 3H R=, F7.3)

      FIQR12=B*AO*AO*F22
      FIQR22=1.0+B*AO*AO*F12
      FIQR2=ATAN(FIQR12/FIQR22)
      FIQR2D=57.29577*FIQR2
      IF(FIQR2D.LT.0.0) FIQR2D= FIQR2D+180.0
      R2=Q/SQRT(FIQR22**2+FIQR12**2)
      WRITE(6,140)  FIQR2D, R2
  140 FORMAT(1X, 26H USING F12 AND F22, PHIQR=, F7.1, 5X, 3H R=, F7.3)

      SECOND DETERMINATION OF DISPLACEMENT FUNCTIONS
      C=Q/R
      A2=B*AO*AO
      COT=COS(PHIQRR)/SIN(PHIQRR)
      ROOT=SQRT(1.0/(1.0+COT*COT))
      DF2=(C/A2)*ROOT
```

```
      DF1=(C/A2)*COT*ROOT-1.0/A2
      WRITE(6,110) DF1, DF2
  110 FORMAT(10X, 5H DF1=, F6.3, 10X, 5H DF2=, F6.3)

      METHOD B
      USING THESE DISPLACEMENT FUNCTIONS CALCULATE AMPLITUDE OF
         VIBRATION AND PHIQX
      UP=DF1*DF1+DF2*DF2
      DOWN1=(1.0+B*AO*AO*DF1)**2
      DOWN2=(B*AO*AO*DF2)**2
      DOWN=DOWN1 + DOWN2
      AMPVIB=Q/(G*RO)*SQRT(UP/DOWN)
      PHI1=-DF2
      PHI2=DF1+A2*UP
      PHI=PHI1/PHI2
      PHIR=ATAN(PHI)
      PHID=57.29577*PHIR
      IF(PHID.LT.0.0) PHID=PHID+180.0
      WRITE(6,120) AMPVIB, PHID
  120 FORMAT(10X, 31H AMPLITUDE OF VIBRATION (INS) =, E10.3, 10X,
     118H PHIQX (DEGREES) =, F6.1//)
  100 CONTINUE
      WRITE(6,30)
   30 FORMAT(1H1)
      STOP
      END
```